Folding Mechanisms

within the

Saltville Thrust Sheet,

Valley and Ridge Province, Tennessee

Presented in partial fulfillment

of the requirements for the

degree Bachelor of Science with distinction.

Department of Geology and Mineralogy

The Ohio State University

June 4, 1990

Christopher H. Swartz

Advisor

Terry J. Wilson

ABSTRACT

Field and laboratory analysis of structures present in an outcrop of a massive carbonate unit within the Ordovician Sevier Shale, located in the Saltville thrust sheet in northeast Tennessee, indicates that folding was produced by a buckling mechanism accommodated by flexural-slip/flow during thrust sheet transport. The modified class 1B geometry of the folds and the kinematic indicators found in the outcrop are consistent with these folding mechanisms. Analysis of timing relations of the structures, as well as comparisons to studies performed on similiar rock units in the vicinity of this outcop, indicate that modification of the folds by a flattening mechanism occurred during thrust sheet transport as well. Greater flattening strain observed in the folds of the southern area of the outcrop compared to those in the northern area can be explained by thrusting on a surface to the immediate south of the southern folds.

Acknowledgements

I would like to thank Dr. Terry Wilson for the large amount of her time spent in advisement of this project. Her help in formulating the initial proposal, gathering of field data, and critique of the drafts is greatly appreciated. I would also like to thank Mrs. Tibbetts for her help in locating the many sources needed to research and complete this thesis, and the Geology Club and the Friends of Orton Hall for financial assistance which defrayed the cost of the thin section cutting and field expenses.

Table of Contents

Table of Figures

Introduction

Continent-continent collision and suturing occurred in the late Paleozoic on the eastern margin of the North American continental plate, producing the Alleghenian Orogeny. A roadcut outcrop of a massive carbonate unit within the Ordovician Sevier Shale, located along U.S. Route 23, approximately two miles south of Kingsport, Tennessee, exhibits folding, faulting and several other significant groups of structures that were produced during this tectonic activity.

The Alleghenian Orogeny resulted in the general northwest transport and deformation of a series of thrust sheets within the Southern Appalachian thrust belt of the Valley and Ridge Province of the United States (Fig. 1). The outcrop is a part of the Bays Mountain Synclinorium contained within the Saltville thrust sheet. The Saltville thrust is positioned approximately in the center of the Southern Appalachian thrust belt (Fig. 2). The outcrop occurs in the cross-strike center of the Saltville thrust sheet, but is slightly closer to the Pulaski thrust to the southeast. The Narrows Thrust sheet is positioned to the northwest of the Saltville thrust (Fig. 3a). In northeast Tennessee, the Copper Creek thrust lies to the northwest of the Saltville thrust (Fig. 3b).

The purpose of this study is to determine the origin of the folding that is exhibited in this outcrop through an analysis of

Fig. 1: Map of the United States with physiographic provinces shown. Valley and Ridge province outlined in red. (Hunt, 1967)

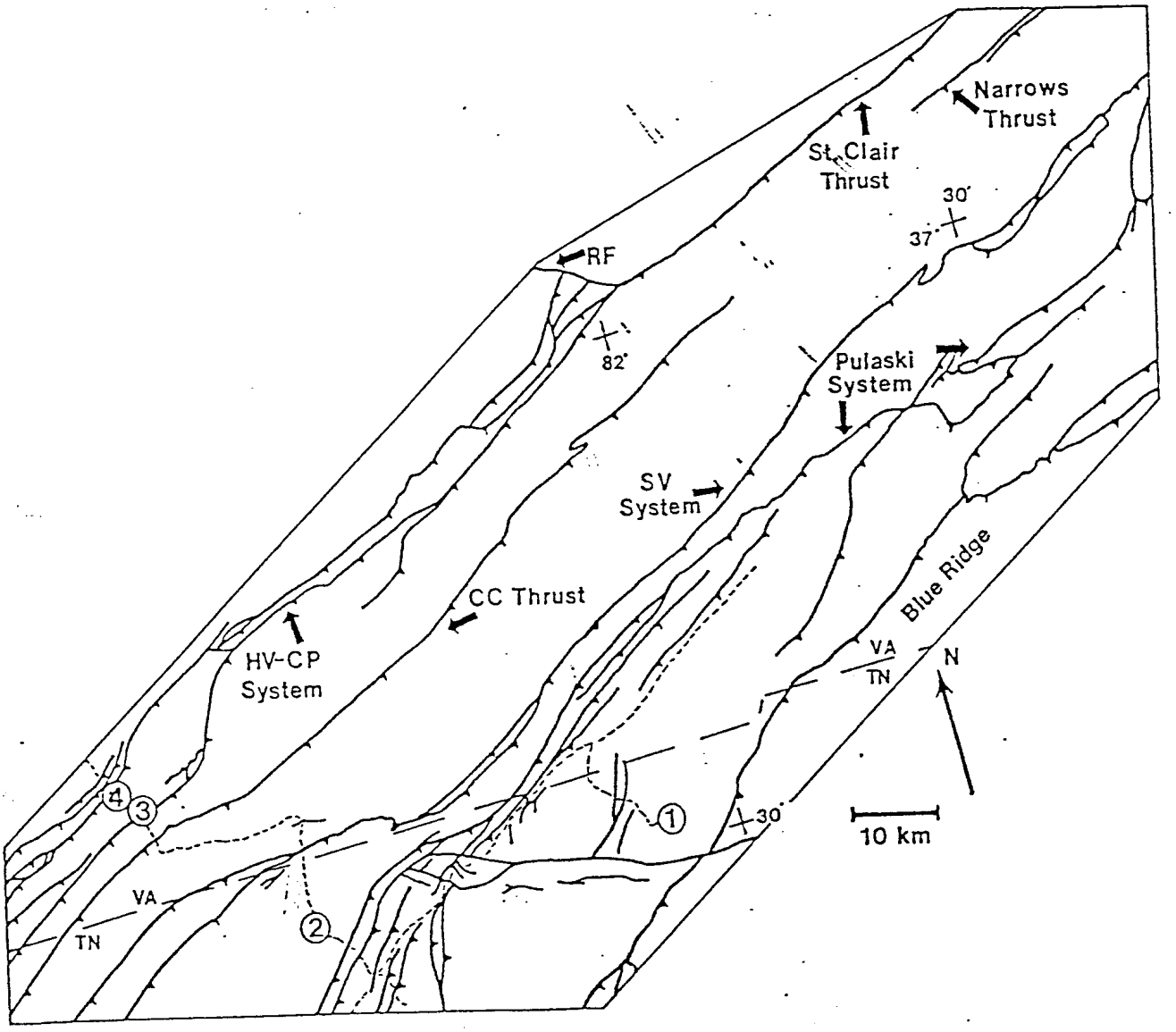

Fig. 2: Map of a portion of the Southern Appalachian Fold and Thrust Belt showing Virginia-Tennessee boundary. Approximate location of outcrop shown with asterisk. SV: Saltville thrust, CC: Copper Creek thrust, HV-CP: Hunter Valley - Cumberland thrust. (Woodward, 1989)

the fold geometry and structural relations between features such as cleavage surfaces, bedding-parallel mineralized veins, mineralized veins at high angles to bedding, and thrust surfaces. These relations were studied in outcrop and in thin sections cut from oriented hand samples gathered at the site. These analyses will determine if the folding occurred as a result of one, or a combination of several, of the following mechanisms:

1) fault propagation folding as part of a ramp-flat trajectory scenario of thrust sheet emplacement (Fig. 4a).

2) simple shear strain within the thrust sheet during transport (Fig. 4b).

3) buckling due to layer-parallel compression initiated prior to thrust transport (Fig. 4c).

4) buckling due to superimposed compressional strain after thrust sheet transport.

The presentation of data pertinent to this study will be in the following manner. A general physical and lithological description of the outcrop will be followed by specific accounts of each of the structural features occurring in the rock unit. A discussion of fold geometry and a general kinematic analysis of motion along bedding surfaces and thrust surfaces will then follow. Finally, a detailed analysis of cross cutting relations among the structural features will be used to construct a full history of the relative timing of formation of the structures. The reconstructed history will then be used as a basis, along with

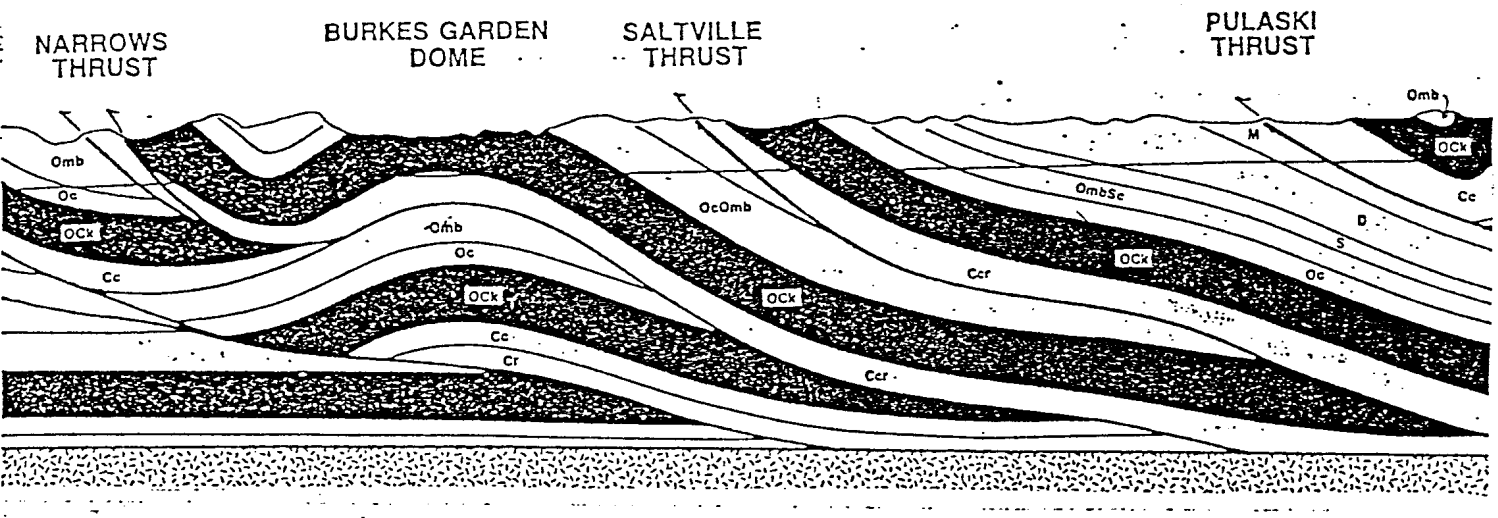

Fig. 3a: Cross section through southern Virginia showing relative positions of the Narrows, Saltville, and Pulaski Thrust sheets . (Woodward, 1985)

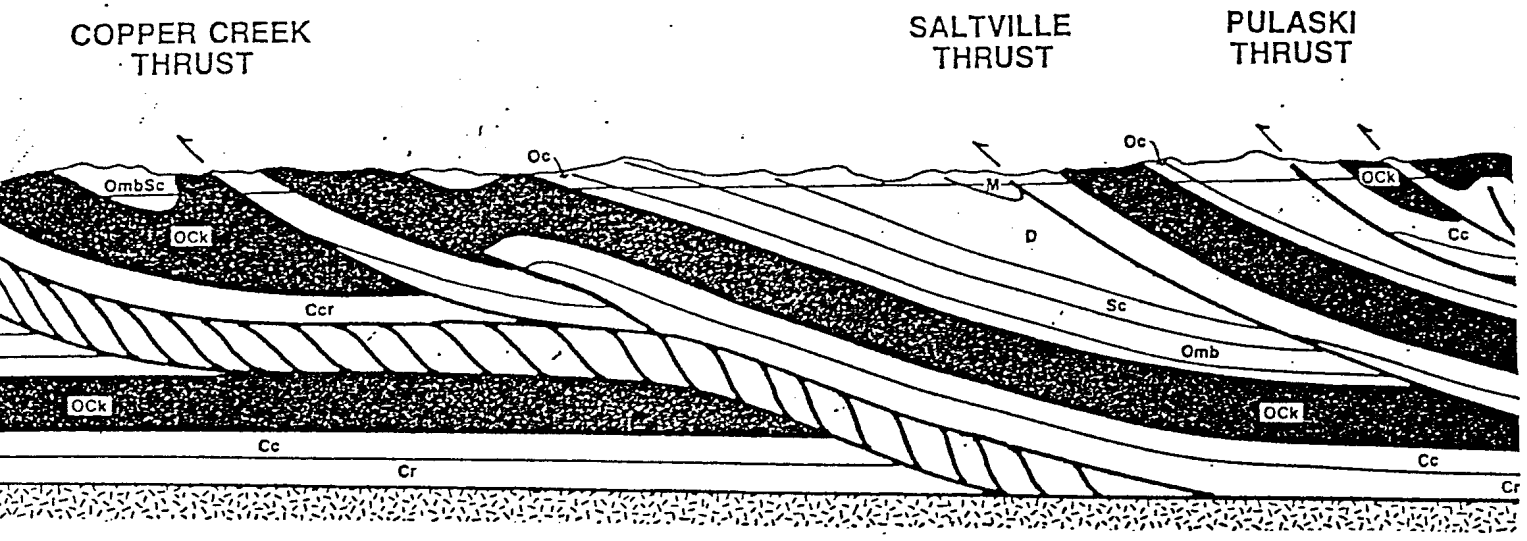

Fig 3b: Cross section through northern Tennessee showing relative positions of the Copper Creek, Saltville, and Pulaski thrust sheets. (Woodward, 1985)

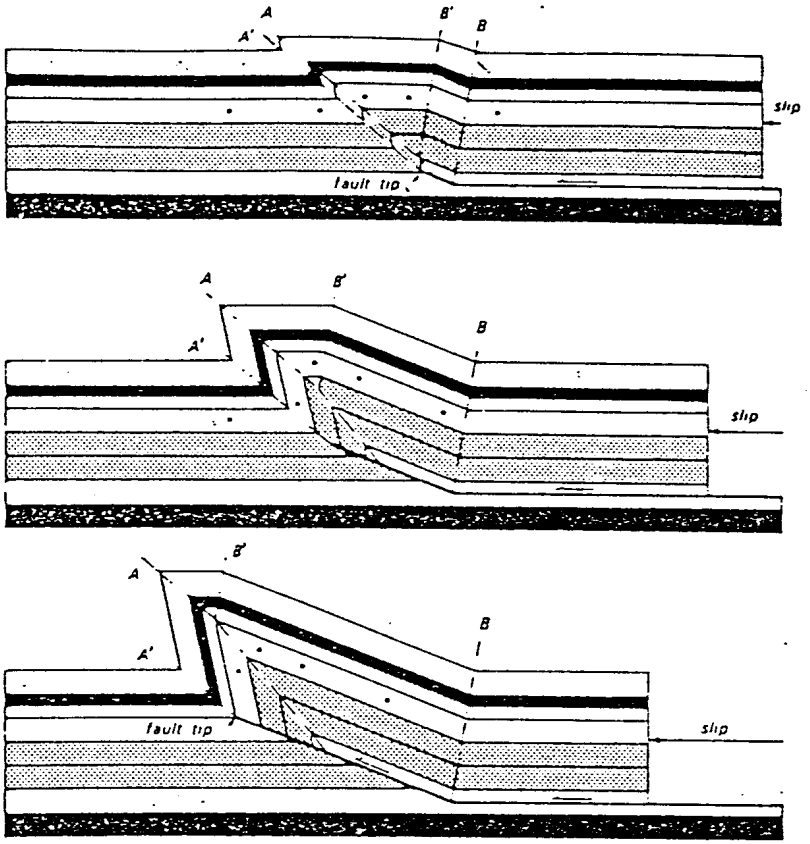

Fig. 4a: Fold development by fault propagation folding. Folding is forced by propagation of fault. (Suppe, 1985)

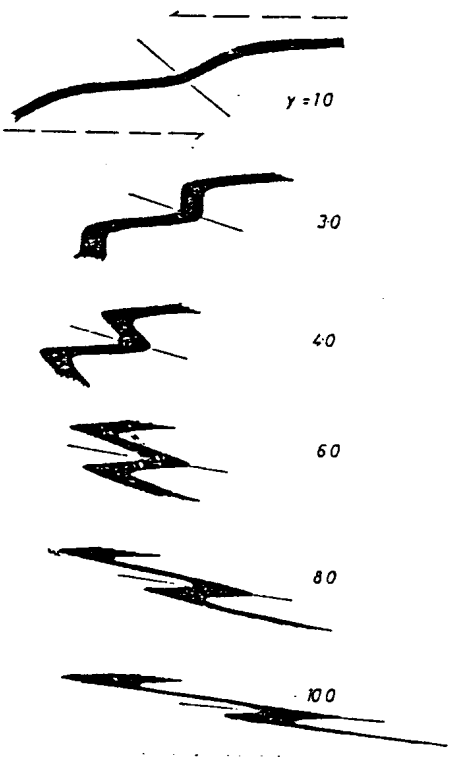

Fig. 4b: Fold development and change in shape by simple shear strain. Arrows indicate sense of shear. (Ramsay, 1983)

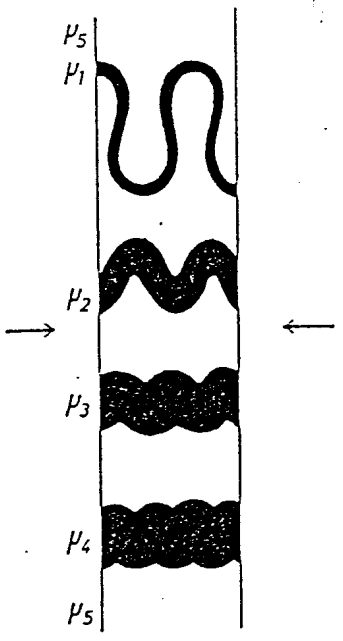

Fig. 4c: Fold development by buckling due to layer-parallel compression. Different wavelengths of folds produced by different thicknesses of the layers are shown. Note maintaining of constant layer thickness. (Ramsay, 1967)

evidence provided by other similar studies in the region, for interpretation of the mechanisms which produced the deformation in this rock unit.

General Physical and Lithological Description

The outcrop occurs on the west side of U.S. Route 23 and is divided vertically into three tiers, each approximately 10 meters high. The first tier extends about one quarter of a mile along the road. The second and third are significantly shorter, and occur only in the northern half of the outcrop (Photo 1).

Original depositional bedding within the rock can be viewed with the naked eye and is fairly consistent throughout the outcrop. It is distinguished by alternating light and dark bands on the order of a few millimeters to several centimeters in thickness. Some bedding thicknesses are greater, being on the order of 10 to 20 centimeters. The bedding surfaces are fairly planar but, if one looks closely, there is much discontinuity. This gives the bedding a lenticular nature.

In hand sample, the rock is very finely crystalline. Slight reflections of light occur off of the faces of the silt-sized quartz grains that are present. The rock is a carbonate and does effervesce readily in hydrochloric acid. No fossil content is visible to the naked eye but, in thin section, fragments of trilobites, brachiopods, and possibly bryozoa were found. The rock is composed of silt-sized, angular quartz and feldspar

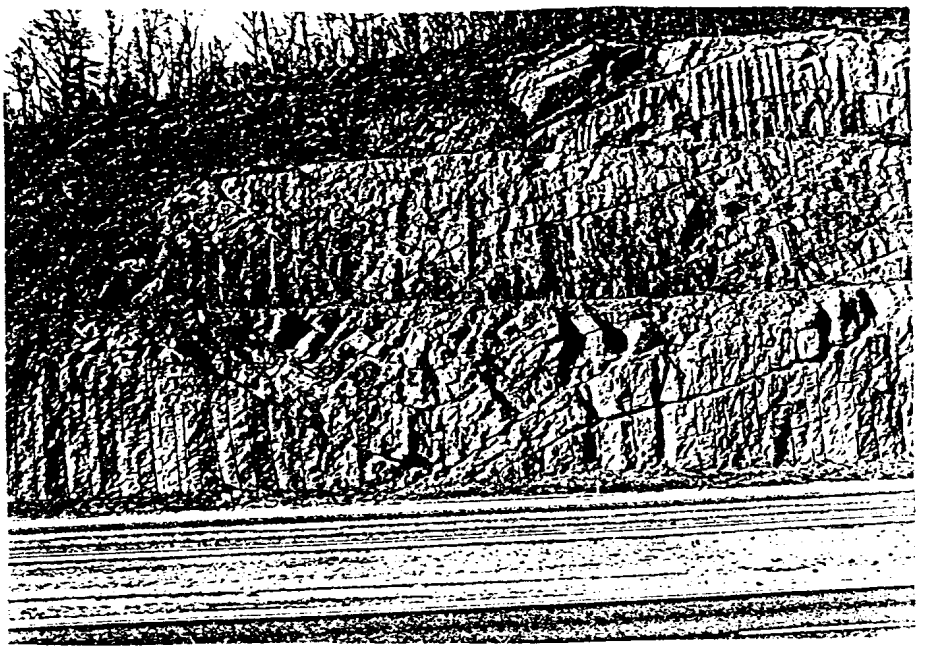

Photo 1: North end of outcrop showing three tiers.

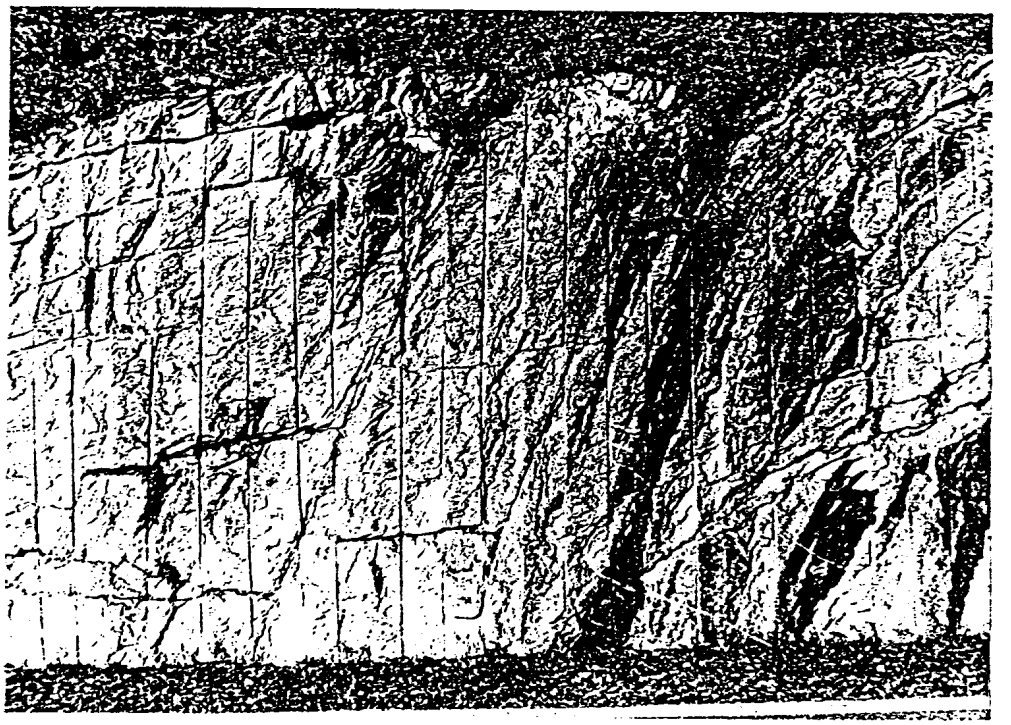

Photo 2: South end outcrop.

grains. These grains occur in a cryptocrystalline, calcareous mud matrix.

The lower portion of the Sevier Shale has been interpreted as having a turbidite-hemipelagic origin (Shanmugan and Walker, 1978). Deposition is thought to have occurred in a deep-water basin formed by rapid subsidence in the early Ordovician.

Folds

Two distinct types of folding appear, one at either end of the outcrop. At the northern end, a series of gentle folds occur. At the southern end a pair of tight, overturned folds occur. In between these two areas of folding, the outcrop is characterized by bedding which dips 20° to 30° NW.

At the northern end, a syncline-anticline-syncline sequence occurs (Profile 1). The layer boundaries that define these folds consist of mineralized and clay-rich surfaces parallel to depositional bedding. Individual layers average 1 to 2 meters in thickness, although some layers .5 meters in thickness occur at random through the folds. The northernmost anticline and syncline of this sequence, to be referred to as folds B and C respectively, are gentle, with an interlimb angle of about 140°. The syncline at the south end of this sequence, to be referred to below as fold A, has an interlimb angle of 100° and is asymmetric to the north. The north limb of fold A develops a shallower dip roughly 5 meters from the hinge zone, changing from 35° SE to 15° SE. From stereographic analysis, the hinge line of folds A, B, and C, was determined to have an orientation of 12°, 238° (Fig. 5). The axial

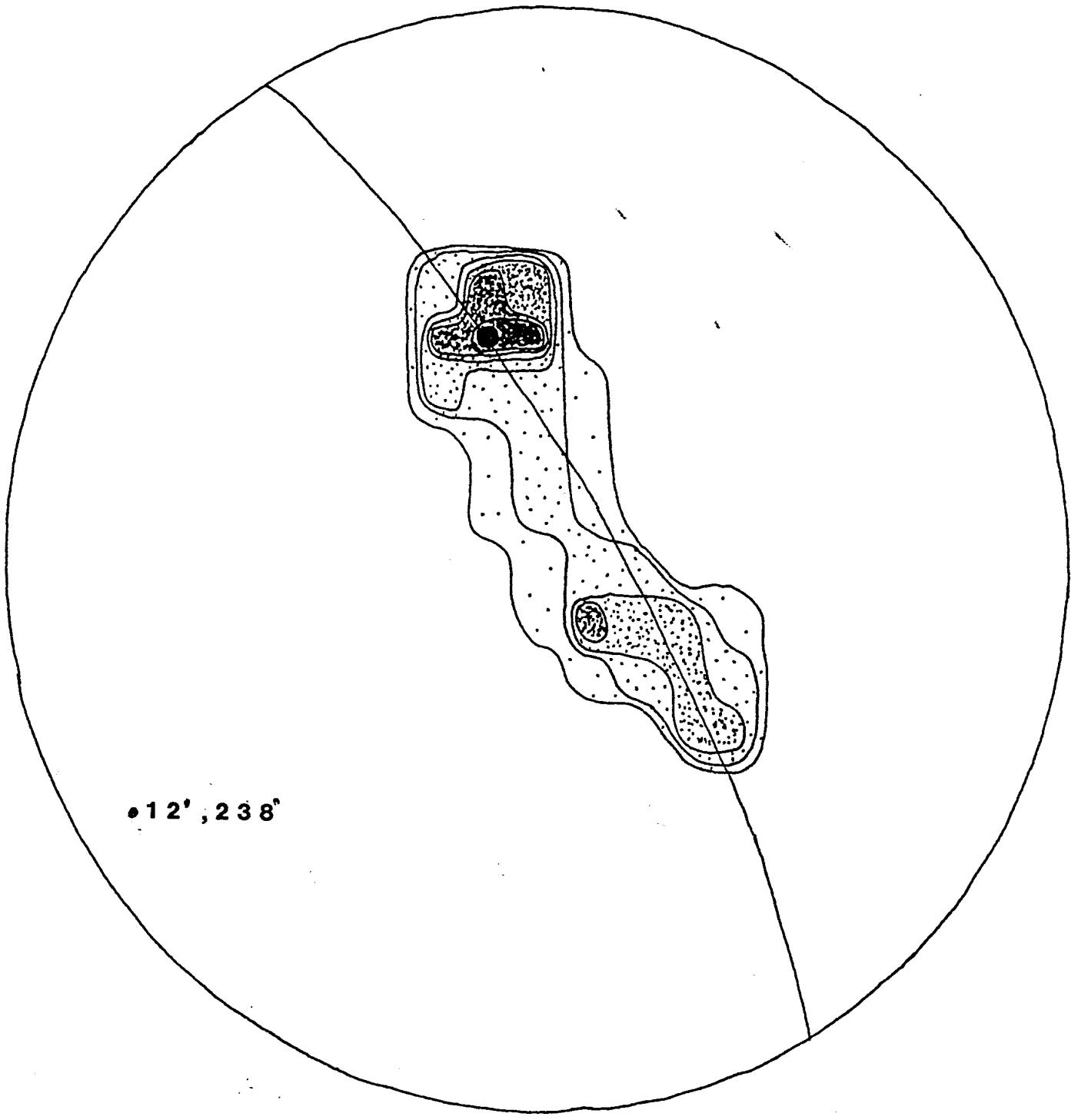

Fig. 5: Contoured stereonet of poles to bedding. Orientation of hinge line of folds A, B, and C indicated.

surface was approximated to strike in the same direction and dip steeply to the northwest.

The second distinct set of folds occurs at the extreme southern end of the outcrop, roughly 100 meters from the first set of folds described above. These folds consist of a tight overturned anticline-syncline sequence, to be referred to below as folds D and E respectively (Profile 2). Each of these folds possesses an interlimb angle of only 50°. Although the lithology and depositional bedding are the same as that at the northern part of the outcrop, the mineralized, bedding-parallel surfaces which define the layers differ from those of that area. Here, the veins are much more closely spaced, occurring every 30 to 50 centimeters.

Another feature of these folds which distinguishs them from the folds to the north is their chevron shape. This shape is characterized by a narrow hinge zone and long planar limbs. Bulbous "saddle reef" structures, consisting of calcitic and clay rich material in the hinge areas of the fold, are also present (Ramsay, 1974).

Sufficient surfaces were not within reach to allow enough measurements to be taken to independently determine the fold axes in this area. From the few orientations which were measured, however, it is assumed the fold hinge line is roughly parallel to that of the northern area. The axial surface dips approximately 60°S.

As stated above, the section of outcrop separating the two

areas of folding is characterized by bedding which dips consistently 20° to 30° NW. This bedding parallels the northwest dipping limb of fold E of the southern area and the northwest dipping limb of fold A in the north area. Also occurring in this region are a number of thrust surfaces.

Veins

There are four types of mineralized veins in the outcrop. One type is oriented parallel to depositional bedding. The second type occurs at an angle of about 90° to the bedding-parallel veins and commonly emanates from these veins. The third type of vein also occurs at an angle of about 90° to the bedding-parallel veins, but they are not physically connected with these vein. The fourth type of vein is also at a high angle to bedding. These veins are several meters in length and cross-cut bedding-parallel veins regularly.

The bedding-parallel veins average 3 cm in thickness and range from .5 to 6 cm in thickness. Most are continuous around the folds. They are filled with calcite characterized by large, blocky crystals with distinct rhombohedral cleavage. There are two distinct components of the bedding-parallel calcite veins that consistently occur together throughout the outcrop. One component consists of blocky calcite layers randomly separated by very thin partings of dark, cryptocrystalline material. These components of the veins are buckled. Occurring with these buckled components are planar layers of blocky calcite which, for the most part, lack these partings. In many areas of the outcrop, these planar

layers truncate the buckled layers. These planar layers also thin near the hinge zone of the folds, not maintaining the same degree of continuity as do the buckled layers.

Both the buckled and planar components of the veins exhibit slickenfiber structures on their surfaces. These calcitic, linear structures are the result of slip between the two rock layers separated by the veins, and parallel the orientation of relative movement between the layers. Direction of motion can be determined if the step-like nature of the slickenfibers is preserved (Fig. 6).

There are two possible origins for this movement along these bedding-parallel veins. Bedding-parallel thrusting, in which the hanging wall moves up and over the footwall, might have occurred previous to folding (Fig. 7). This mechanism would have created lineations recording movement in one direction along the now folded surfaces. Flexural slip could also have produced lineations on the vein surfaces. This type of movement would have occurred concurrently with folding, acting to accommodate folding by movement of the limbs relative to each other to accommodate compression and development of the fold (Fig. 8). Lineations produced by flexural slip would be expected to record a sense of movement toward the hinge on each limb and would be absent in the hinge zones, where no movement occurred during folding.

It must be stated that the buckled and planar components of the bedding-parallel veins do not have to record the same mode of movement. In fact, the differences in appearance and continuity

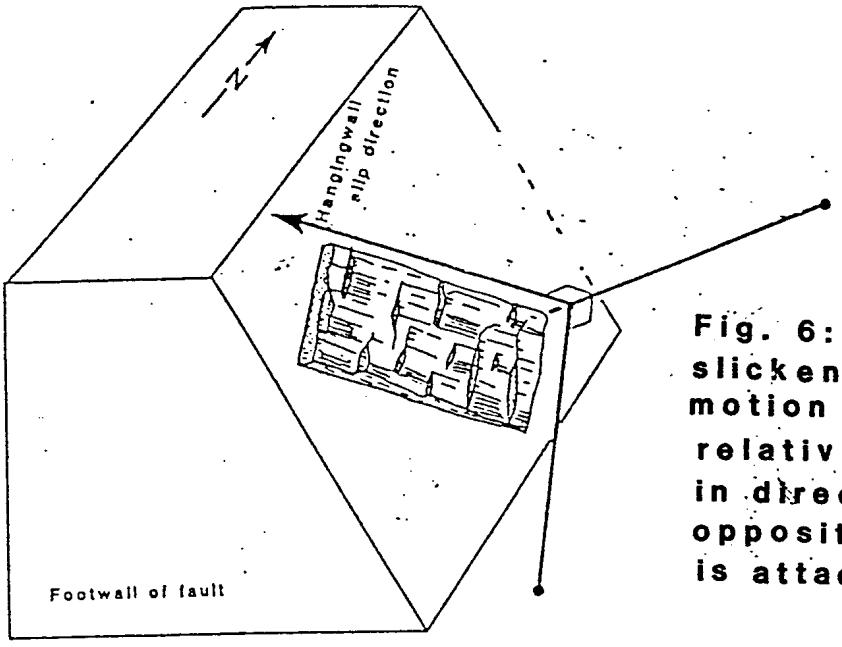

Fig. 6: Stepped nature of calcite slickenfibers used to determine motion direction of hangingwall relative to footwall. Steps point in direction of motion of block opposite to the one to which it is attached. (Marshak and Mitra, 1988)

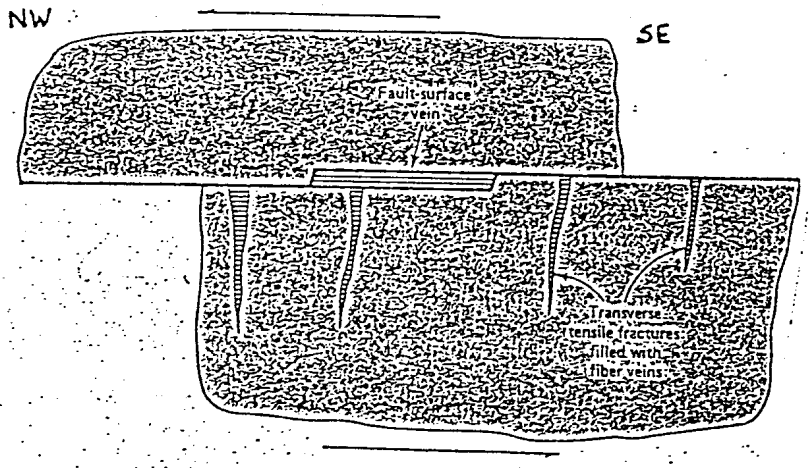

Fig. 7: Diagram depicting bedding-parallel thrusting and creation of extension veins perpendicular to bedding parallel veins. Note hangingwall motion toward northwest. (Suppe, 1985)

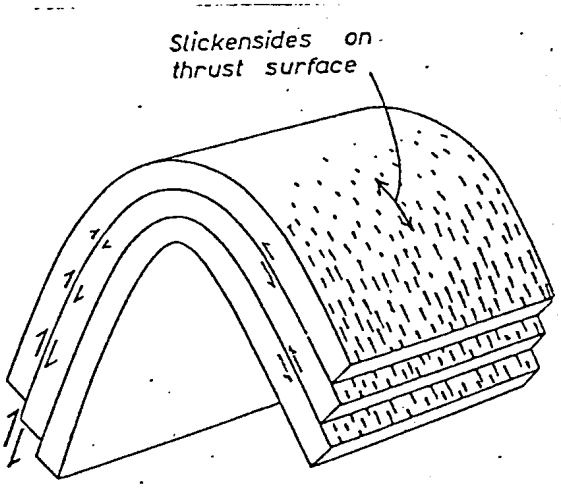

Fig. 8: Diagram depicting accommodation of folding by flexural slip. (Ramsay, 1967)

exhibited in the planar layers with respect to the buckled ones, as well as the truncation of the buckled layers by the planar layers, indicates they were not formed at the same time. These two components of the bedding-parallel veins represent two entirely different slip events and possibly two different modes of movement as well. Evidence to correlate these components with their respective movement origins will be presented below.

In two specific sites in the outcrop, planar, bedding-parallel calcite veins occur with an increased frequency relative to the surrounding areas. One site is at the bottom of fold A near the hinge zone in the south-dipping limb (Profile 1: A). An array of these veins occur in the southeast-dipping limb of the fold. These veins range in length from 30 cm to 1 meter and die out near the hinge of the fold. This same phenomenon occurs near the bottom of fold E in the outer arc of the north-dipping limb (Profile 2: A). These veins also die out near the hinge.

Another group of mineralized veins occurs at an angle of 90 to bedding. These veins emanate from the bedding-parallel veins, suggesting that they formed at the same time. They range in length from a few centimeters to 1 meter. Many of the veins which emanate from the bedding-parallel veins contain angular fragments of country rock (Photo 3). These veins maintain a uniform perpendicularity with the bedding-parallel surfaces and occur with regular frequency in both the limbs and the hinge zones of the folds of the northern and southern areas.

The third type of vein also occurs in both areas, but are

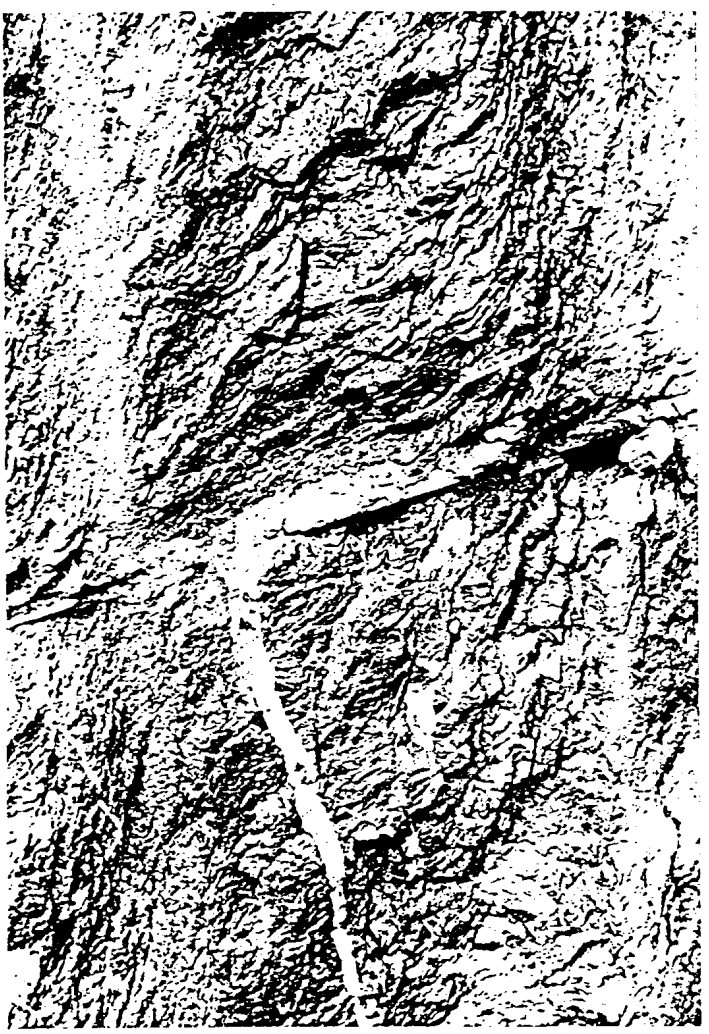

Photo 3: Extension vein containing fragments of country rock. This vein emanates from a bedding-parallel vein.

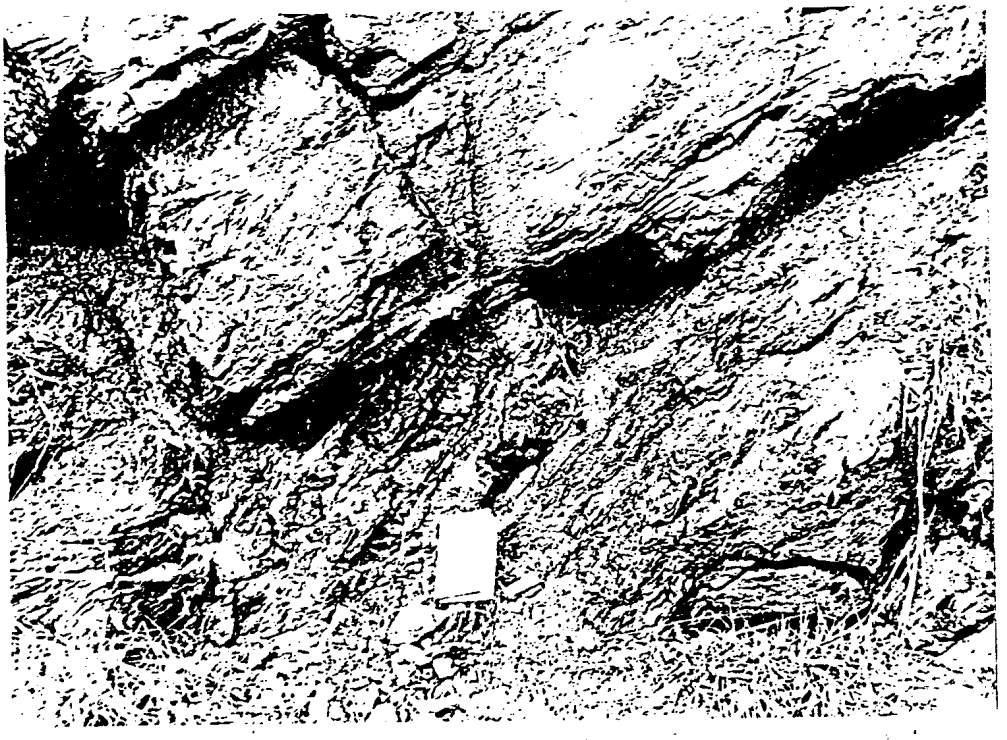

Photo 4: Block of discordant bedding (above book). Thrust surface extends up and to the right.

more common in the northern folds. These veins are characterized by a vaguely sigmoidal shape and do not come into contact with the bedding-parallel veins. No fragments of country rock were seen in veins of this type.

The fourth type of mineralized vein occurs at a relatively high angle to bedding (>60°) and regularly cuts across the bedding-parallel veins. These veins occur in the northern folds, although they differ in their relation to one another in the first and second tiers. In the first tier, these veins occur near the hinge zone of fold A in a parallel array in the south-dipping limb (Profile 1: B). These veins extend for several meters and have an average thickness of 1 to 1.5 cm. They dip generally 65°SE and crosscut bedding-parallel surfaces. Slickenfibers were not observed on the surfaces of these veins. In the second tier, these veins commonly occur in sets which crisscross each other (Profile 1: C). They dip both northeast and southwest in a range of 30° to 40° . They range in length from 1-2 meters to 5 meters and have an average thickness of 1.5 to 2.0 cm. Slickenfiber lineations were observed and measured on two of these surfaces.

Thrusts

There are several surfaces in the outcrop along which motion has occurred, but which are not calcite-filled veins. One such surface occurs along the southeast-dipping limb of fold A (Profile 1: D). This surface appears at ground level near the hinge zone of the fold and contains an abundance of clay material. It is along this surface, near the top of the first tier, where

displacement of layers of the fold can be observed (Profile 1: E). The upward to the north sense of motion of the hangingwall allows this surface to be classified as a thrust fault. Near the hinge of fold A, there exists a rectangular block of Sevier Shale roughly 30 centimeters by 60 centimeters which has bedding discordant to that of the surrounding rock (Photo 4), (Profile 1: F). The bedding within the horse has an orientation of 258°, 56° SE, whereas the bedding in the limb of the fold adjacent to the horse has an orientation of 250°, 37° SE. The thrust surface occurs between this block and the the bedding of the southeast limb of the fold and travels up the limb parallel to bedding. Near the inflection point where the limb changes curvature, the thrust deviates from its bedding-parallel trend and continues at an angle of dip of approximately 40° SE. It is here that the thrust surface begins to truncate bedding.

Another similar surface occurs several meters below the first and follows an orientation roughly parallel to it (Profile 1: G). This surface continues up into the second tier, cutting through the northeast-dipping limbs of the anticline. No displacement of bedding was viewed near this surface, but the steps of the slickenfibers observed on the surface indicated the hangingwall moved up to the north.

Two other surfaces worthy of mention occur in the southern section of the outcrop. Here, a fracture surface with no apparent mineralization traverses the axial plane of fold E and dips 35° SE (Profile 2: B). No displacement of bedding was observed along

this surface. Also, a major thrust surface parallel in dip to the one above occurs just south of the inner core of fold D (Profile 2: C). Movement along this surface has caused obvious displacement of bedding in the southeast-dipping limbs of the anticline. This displacement indicates the hangingwall moved up to the north. Downwarping of bedding in close proximity to the thrust surface can be seen also (Profile 2: D).

Cleavage

Smooth cleavage surfaces are penetrative in outcrop and hand sample. Surfaces are spaced an average of 5 to 10 millimeters apart. An area of intense cleavage occurs in the middle of the outcrop between the two sections of folding. Here, a zone roughly 10 meters wide occurs in which the cleavage is spaced only 1 to 2 millimeters apart. Some cleavage surfaces can be traced for 1 meter or more.

In the northern section, the occurrence of cleavage is uniform in intensity in the hinge zone and in the limbs. The orientations of the surfaces are also fairly consistent in strike. A density diagram of 30 poles to cleavage surfaces occurring throughout the outcrop is presented in Figure 9. The large cluster in the northwest and southeast quadrants represents the southeast and northwest dipping surfaces, respectively, of the cleavage of the northern area. The cluster of greatest density corresponds to the southeast dipping cleavage surfaces, which are roughly parallel in strike to the axial surfaces of folds A, B, and C. Opposite dips on opposite limbs of the folds and the

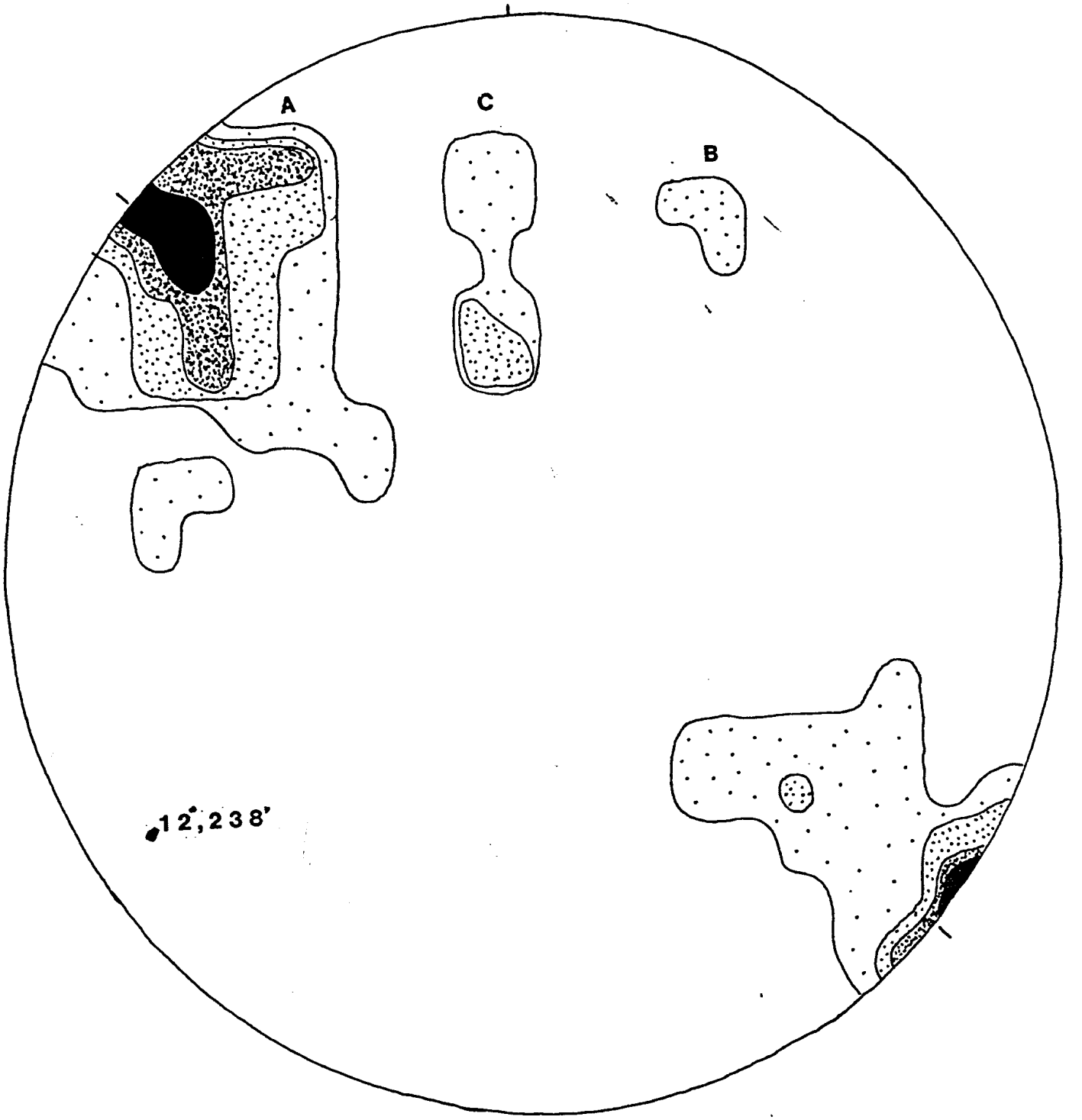

Fig. 9: Contoured stereonet of poles to cleavage measured in (A) - folds A, B, and C, (B) - block of discordant bedding, and (C) - folds D and E. Hinge line of folds indicated.

dispersion in dip shown by the elongation of the cluster results from a fanning arrangement with respect to the axial surface. This fanning arrangement indicates that a population of cleavage surfaces formed prior to folding.

This divergent nature was observed in outcrop. In the hinge areas of the folds, cleavage remained close to vertical, dipping at angles of 75° SE, 90° SE, and 85° N. In the limbs, however, dips of 43° SE, 66° SE, and 63° NW were measured. The fanning nature of a population of cleavage in the folds in the north area is an important factor in determining the timing of cleavage development relative to fold initiation and will be discussed further below.

The cluster of poles designated as "C" in Figure 9 represents, in part, a population of cleavage surfaces measured in the folds of the south area. The cleavage in the southern folds is characterized by greater intensity in hinge zones relative to the limbs and is axial planar in orientation. The general orientation of the this cleavage is 260°, 60° SE.

The small cluster in the northeast quadrant (B) represents poles to surfaces measured in and near the block of disconcordant bedding near the hinge of fold A. The orientation of cleavage in the block is 301°, 62° SW. The inconsistency in orientation of the cleavage relative to that of the cleavage in the rest of this area can be readily seen in Figure 9 and indicates reorientation of cleavage by block rotation during thrusting.

In thin section, the cleavage surfaces are spaced an average of a few millimeters apart and appear as dark seams which cut

through the cryptocrystalline matrix of the rock. Where these seams come in contact with groupings of quartz and feldspar grains, the seams are deflected around them. There are many areas where the seams cut through microscopic calcite veins and fossil fragments, causing an apparent displacement in them. This cross-cutting and apparent displacement by the cleavage surfaces can also be seen in outcrop. For example, truncation and displacement of the buckled veins and sigmoidal tension gashes by cleavage seams passing through them was observed.

These observations, made both in thin section and outcrop, indicate the formation of the cleavage surfaces was by pressure solution. Pressure solution is a mechanism by which diffusive mass transport of rock material occurs in an aqueous environment through solution and reprecipitation. A chemical potential gradient is set up by stresses acting differentially on certain planes within the rock mass. This chemical potential gradient drives the transport of dissolved material along cleavage surfaces away from areas of high stress. This material is redeposited in areas of lower stress. Materials that are insoluble, such as clays, are left along the seams. This residual material is what allows the cleavage seams to be observed in thin section and outcrop. The apparent displacement of structures discussed above is due to a loss of volume by this transport mechanism. The large number of calcite veins in the rock acted as sinks for the redeposition of this transported material.

Fold Geometry

Orthogonal thickness studies after Ramsay (1967) were done on fold profile sections of the folds in the outcrop. The fold profile sections were created by tracing bedding-parallel calcite veins which appear in the photographs taken. These veins provide a visible means of distinguishing the fold curvature in the photographs. In fold A, six layers were distinguished. These layers were designated A1, A2, etc. (Fig. 10). Folds B and C were not studied due to the distortion present in the photographs and because of the limited data which can be derived from such gentle folds. Three layers in Fold D were traced and were designated D1, D2, and D3 (Fig. 11). Four layers were traced in fold E and were designated E1, E2, E3, and E4 (Fig. 12).

The thickness studies were done in order to determine in which class, or classes, the folds of this outcrop might be placed with respect to the classification scheme presented by Ramsay. Classifying the folds of this outcrop according to this classification scheme will provide information on the folding mechanisms which produced them. This classification is based on three end member classes of fold shape.

Class 1 folds are characterized by a greater curvature change in the inner arc relative to the outer arc of a layer (Fig. 13). There are three subclasses of class 1 folds. In class 1A folds, the orthogonal thickness of the limbs exceeds that of the hinge. In class 1B folds, the orthogonal thickness is constant throughout

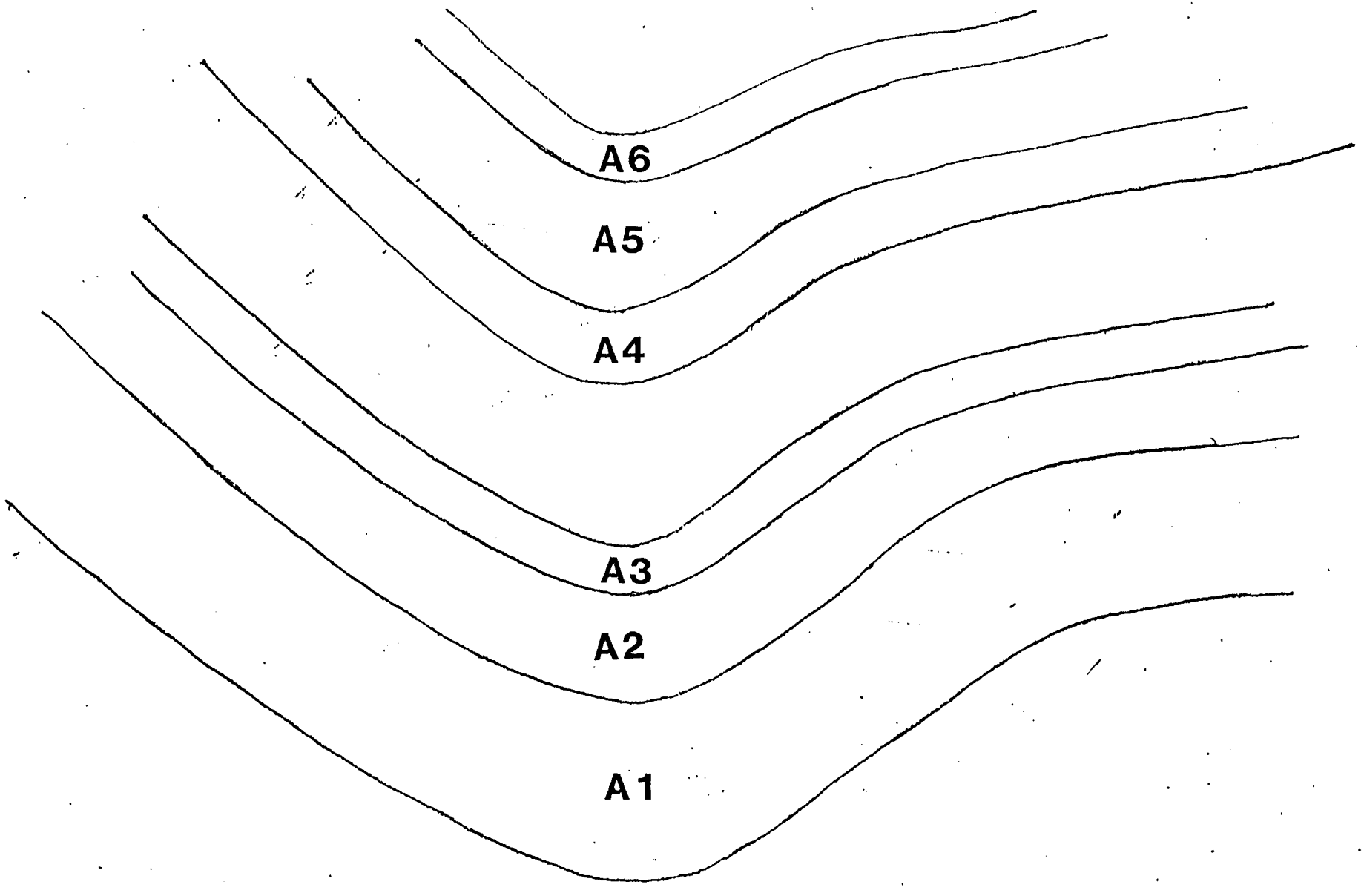

Fig. 10: Profile of fold A with layer distinctions shown.

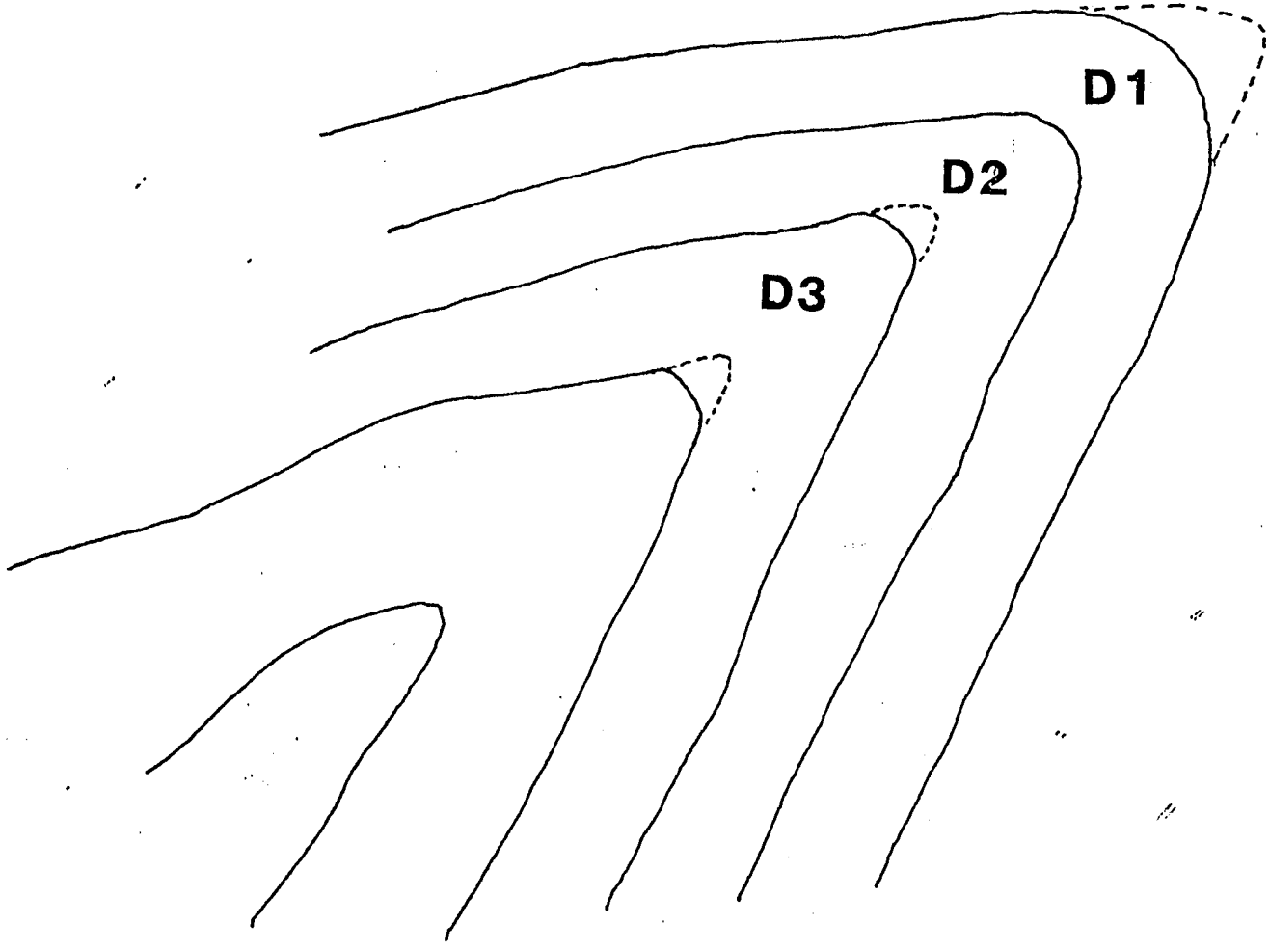

Fig. 11: Profile of fold D with layer distinctions shown.

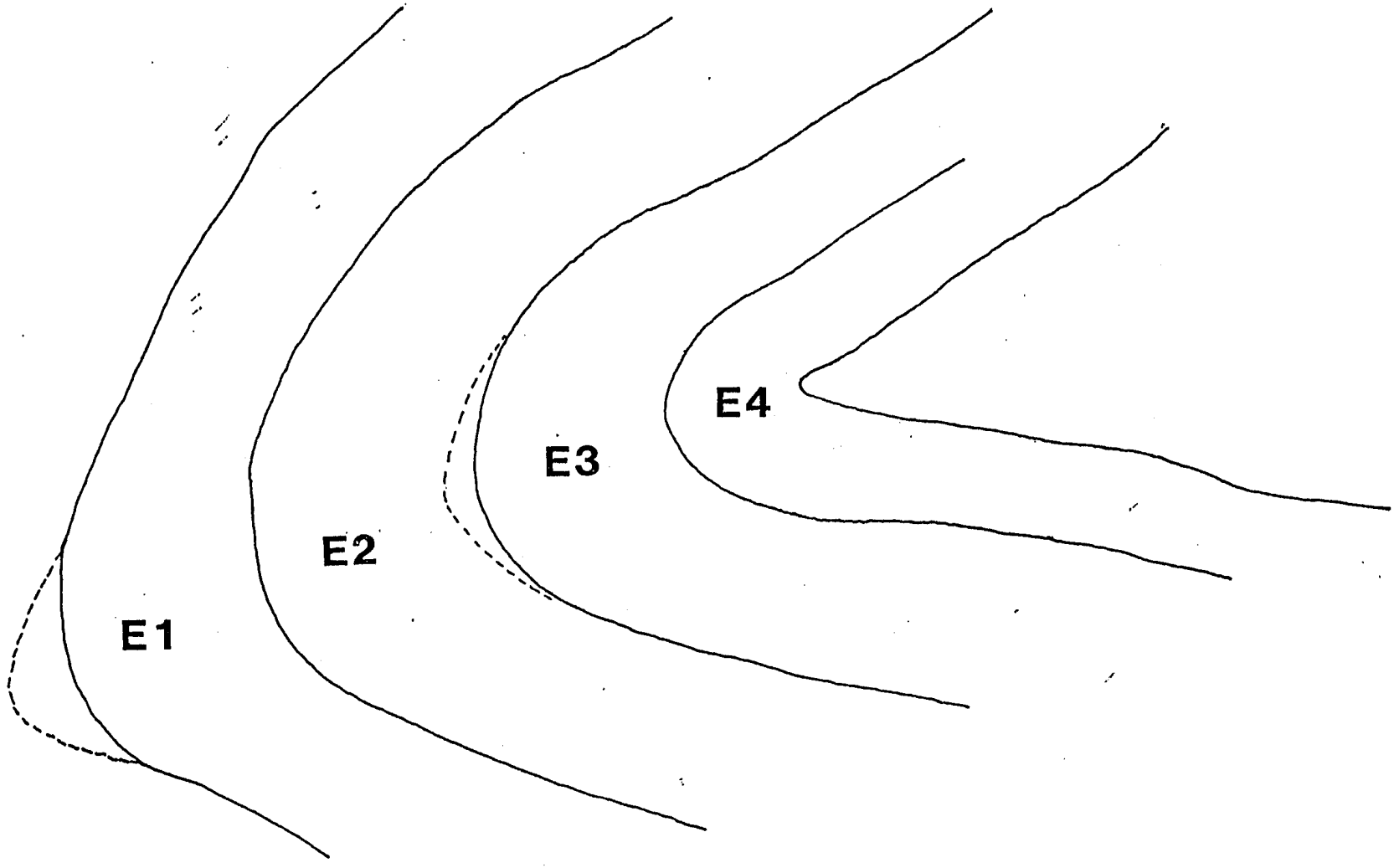

Fig. 12: Profile of fold E with layer distinctions shown.

the limbs and hinge. In class 1C folds, the orthogonal thickness of the limbs is less than that of the hinge.

Class 2 (similar) folds are characterized by identical curvature of the inner and outer arcs of a layer (Fig. 13). Thus, the layers of similar folds have the same shape. The thickness measured parallel to the axial surface trace of a layer is constant for class 2 folds.

In class 3 folds, the rate of change of curvature of the outer arc is greater than that for the inner arc (Fig. 13). Thickness measured parallel to the axial surface trace of a layer is always less than that for the hinge.

It has been determined by experimental studies of rock deformation that certain mechanisms of folding produce these differing classes of folds. One mechanism shown to produce Class 1B folds is layer-parallel compression, or buckling. Class 2 folds are produced by modification of original class 1B folds by an infinite amount of flattening. Class 1C folds are intermediate between class 1B and class 2 end members and are also produced by modification of a class 1B shape by a flattening mechanism (Ramsay, 1967).

The studies consisted of constructing tangent lines to the limbs of the layers of the folds at a series of apparent dip angles (α) (Fig. 15). The orthogonal thickness (t_α) between the tangent lines to the two surfaces comprising a layer was measured for a series of α values. The t_α values were then divided by the orthogonal thickness at the axial plane trace (t_o) to obtain the

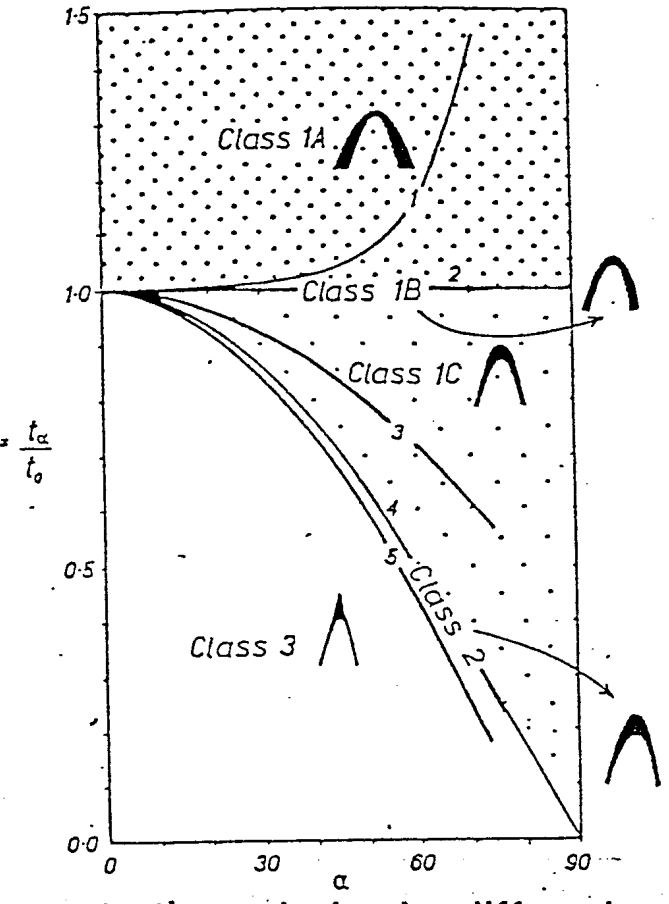

Fig. 13: t' graph showing different fields representing the classes of folds. Folds depict limb thickness relative to hinge and relative curvature of inner and outer arcs for each class. (Ramsay, 1967)

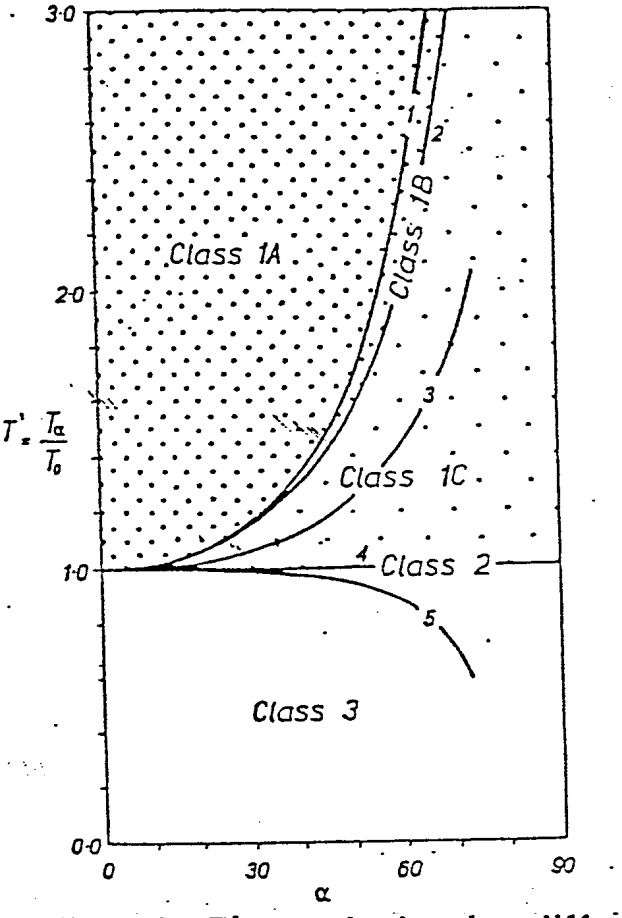

Fig. 14: T' graph showing different fields representing the classes of folds. (Ramsay, 1967)

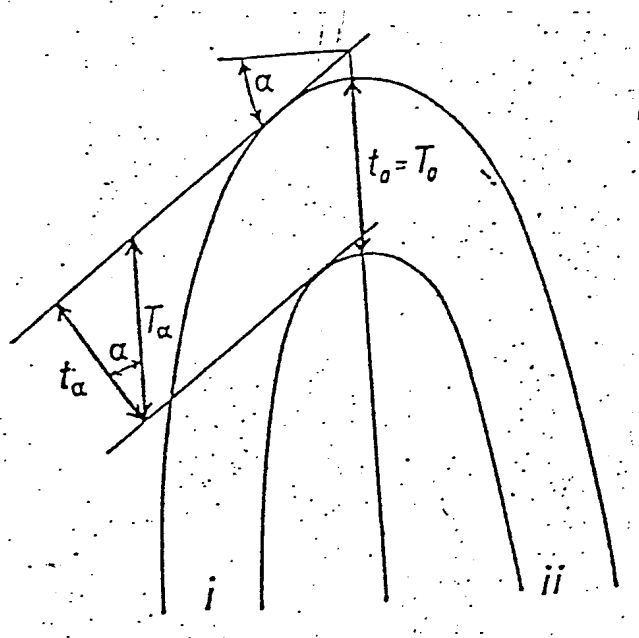

Fig. 15: Diagram showing construction of tangent lines at an apparent dip and geometric relationships of t_α and T_α. (Ramsay, 1967)

ratio t'_{α}. These values of t'_{α} were then plotted against apparent dip (α) for all layers in each limb of the folds on a graph that is divided into fields representing the classes of folds described above (Ramsay, 1967) (Fig. 13). In a t'_{α} versus α graph, the class 2 curve is calculated based on the relationship $t'_{\alpha} = \cos\alpha$, and the class 1 line is constant at a value of 1.

The thickness parallel to the axial plane trace (T_o) was also measured at each of the apparent dips (Fig. 15). The ratio (T'_{α}) of T_{α} to $T_o = t_o$ was then plotted against the apparent dip. In this graph the fields representing the classes of folds are reversed from that of the t'_{α} graphs (Fig. 14). Thus, the class 2 line is now constant at a value of 1, and the class 1B curve is calculated from the relationship $T'_{\alpha} = \sec\alpha$. For both the t'_{α} and the T'_{α} graphs the class 1C field is divided into increments of 10% representing a range of amount of flattening from 1% to 100% (Fig. 16a,b).

The t'_{α} and T'_{α} graphs values are two methods of representing the same geometric relationship exhibited in the hinge and limbs of a layer (Fig. 15). The two different plots for a single layer should then produce similar results. By using both methods of graphing, more data is available to make comparisons and draw conclusions with.

The T'_{α} and t'_{α} graphs of the layers of fold D produced distinctive trends (Fig. 17,18). In both types of graphs, all layers except for D1 plotted in the class 1C field. Also, increased flattening was reflected in the plots for the layers

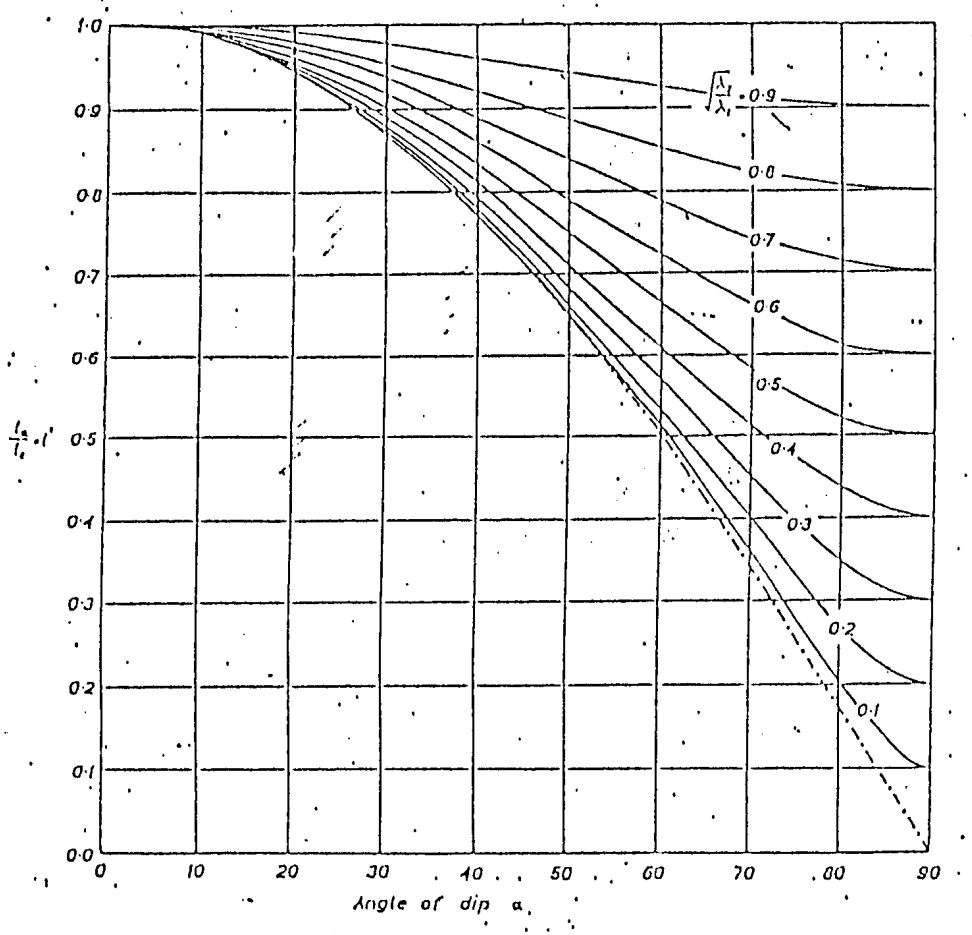

Fig. 16a: t'_α graph showing division of class 1C field into increments of 10%. (Ramsay, 1967)

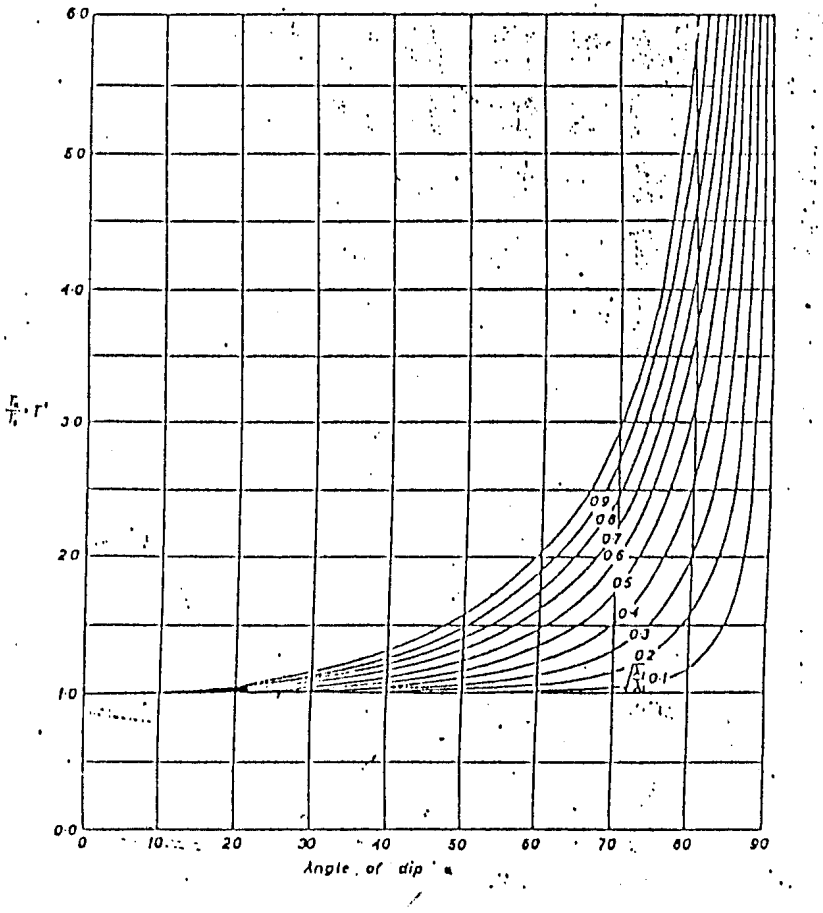

Fig. 16b: T' graph showing division of class 1C field into increments of 10%. (Ramsay, 1967)

Table 1

Fold	Layer	Graph	Percent Overturned	Flattening Normal limb
D	D1	t'	10%	30%
	D2		45%	60%
	D3		80%	75%
	D1	T'	Class 1A	5%
	D2		45%	40%
	D3		70%	60%
E	E1	t'	Class 2, 50% at 40°	Class 3
	E2		35%	35%
	E3		70%	50%
	E4		75%	Class 1B until 30°, then 25%
	E1	T'	30%	Class 3
	E2		5%	20%
	E3		30%	20%
	E4		35%-40%	Class 1A

Table 1: Tabular summary of the results of geometric analysis.

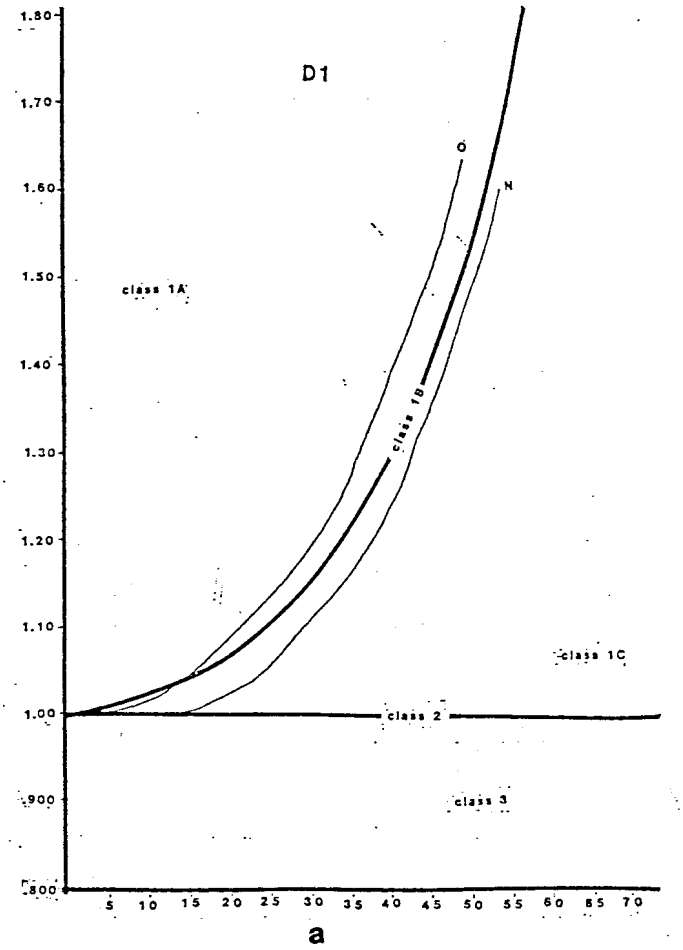

a

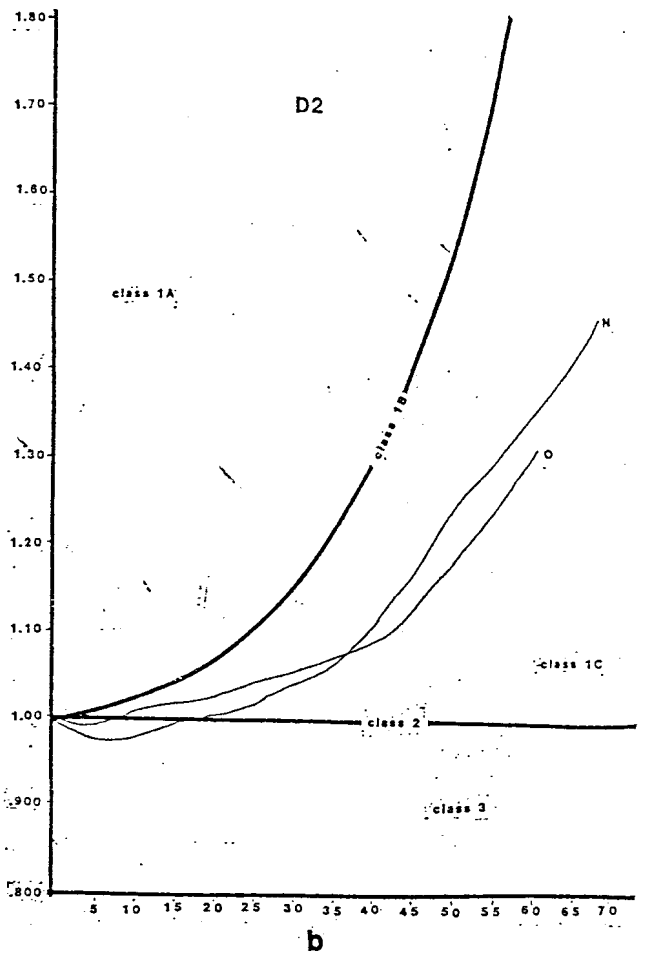

b

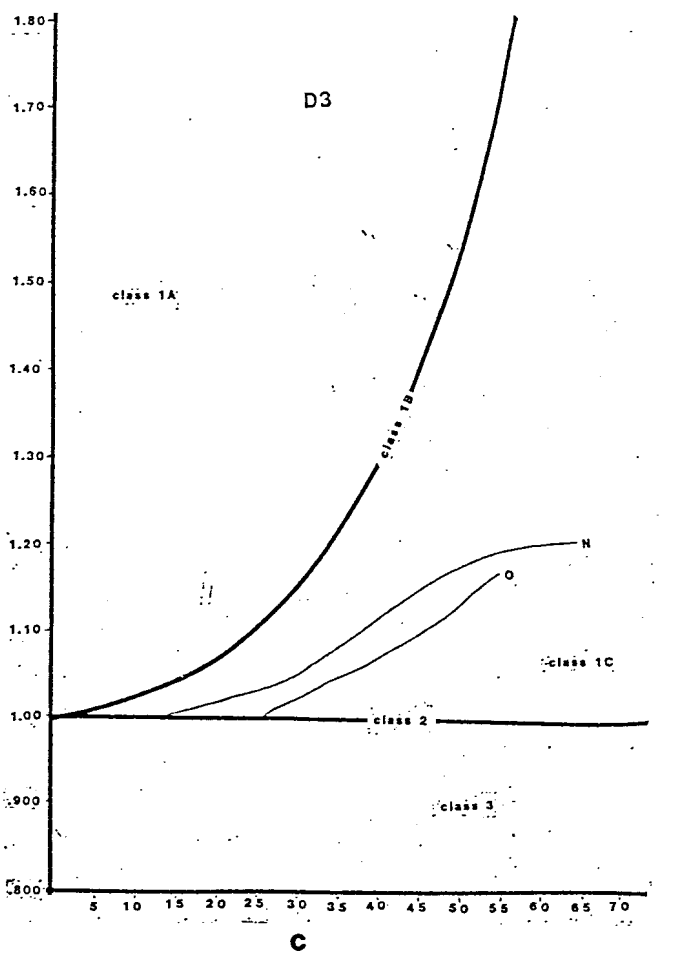

c

Figs. 17 a,b,c: T' graphs for fold D. "N" represents normal limb, "O" represents overturned limb.

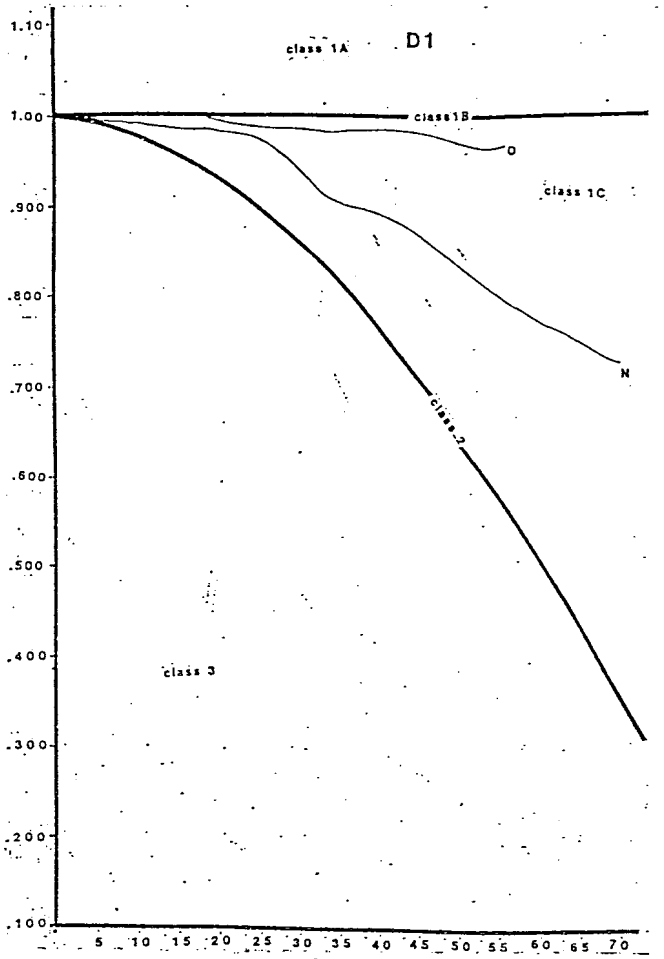

d

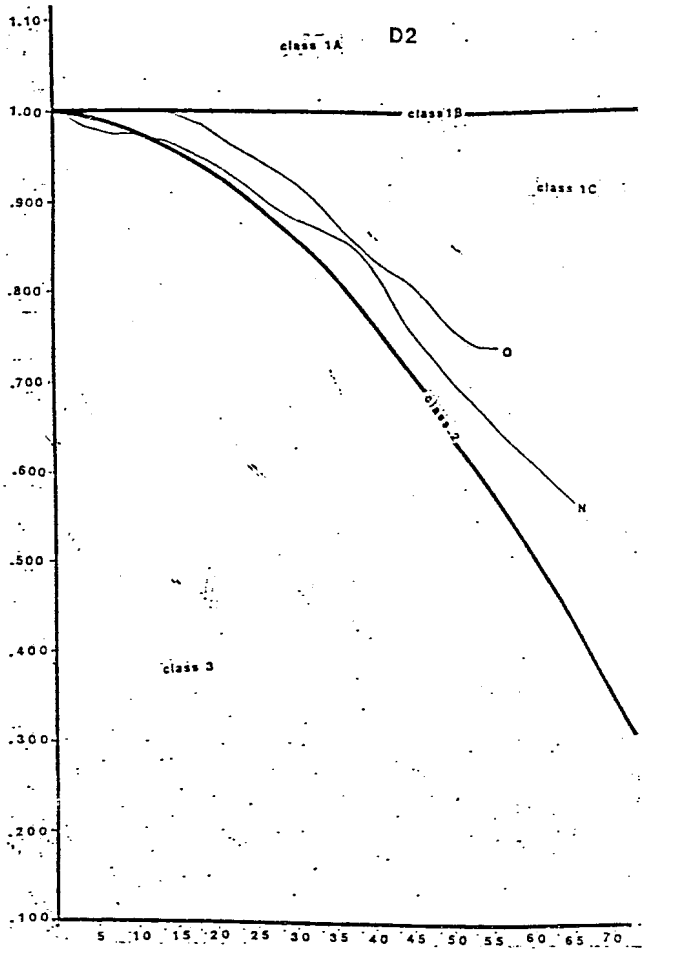

e

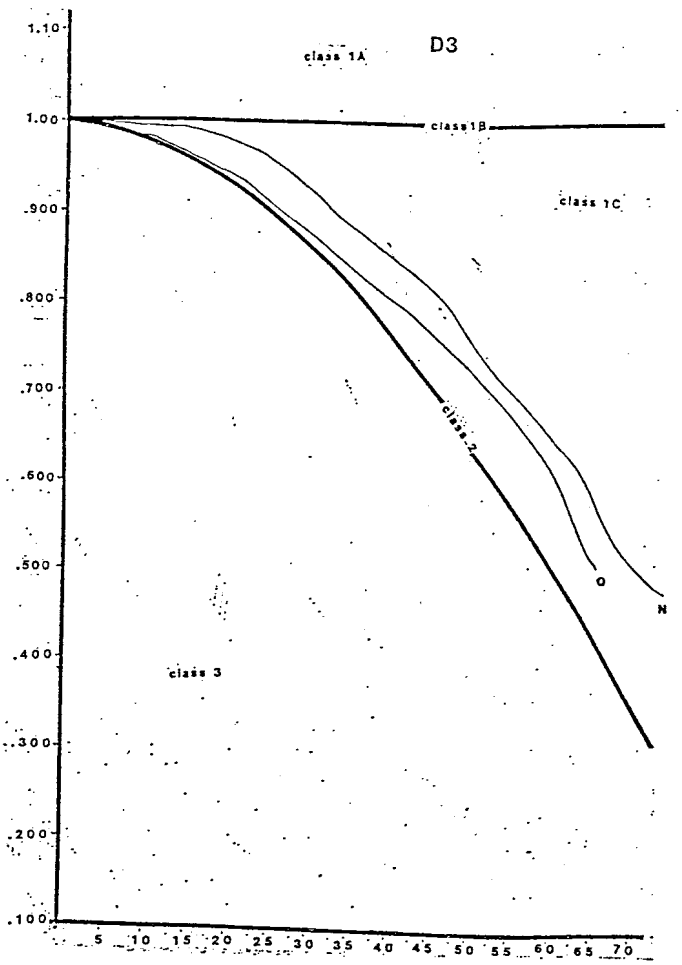

f

Figs. 17 d,e,f: t'_{∞} graphs for fold D.

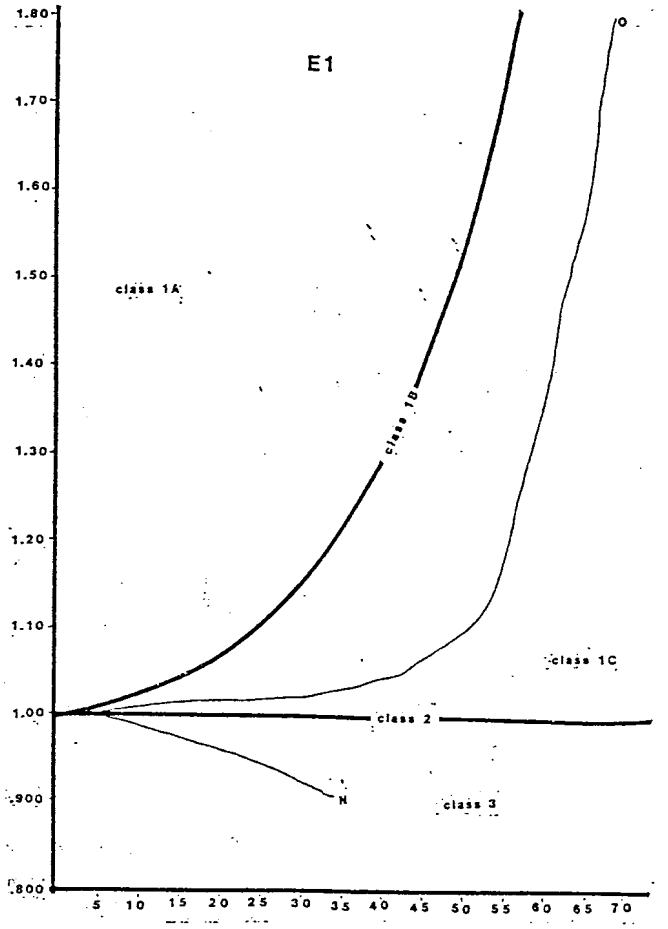

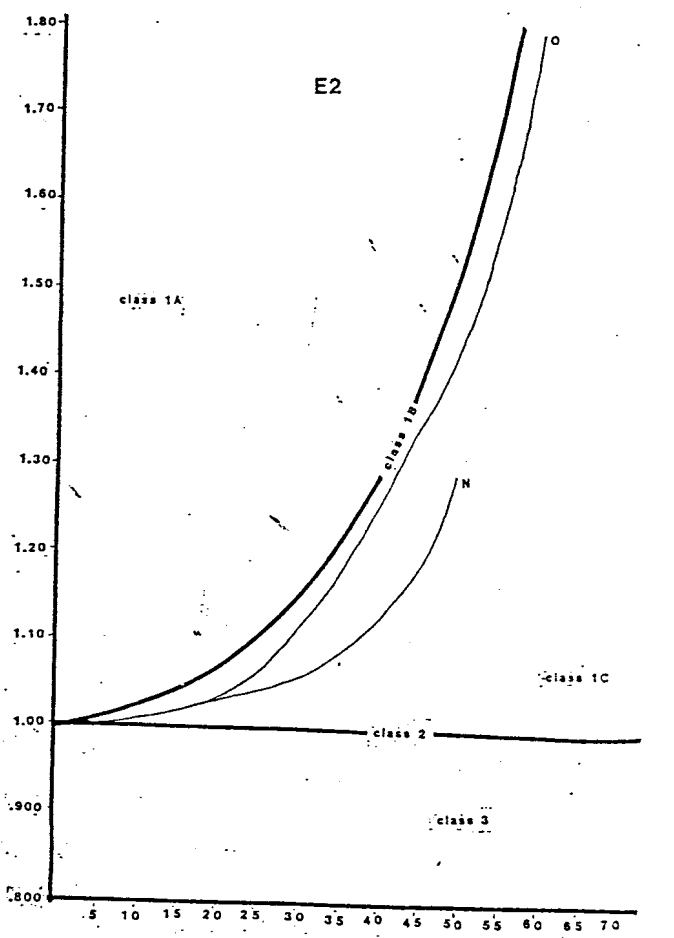

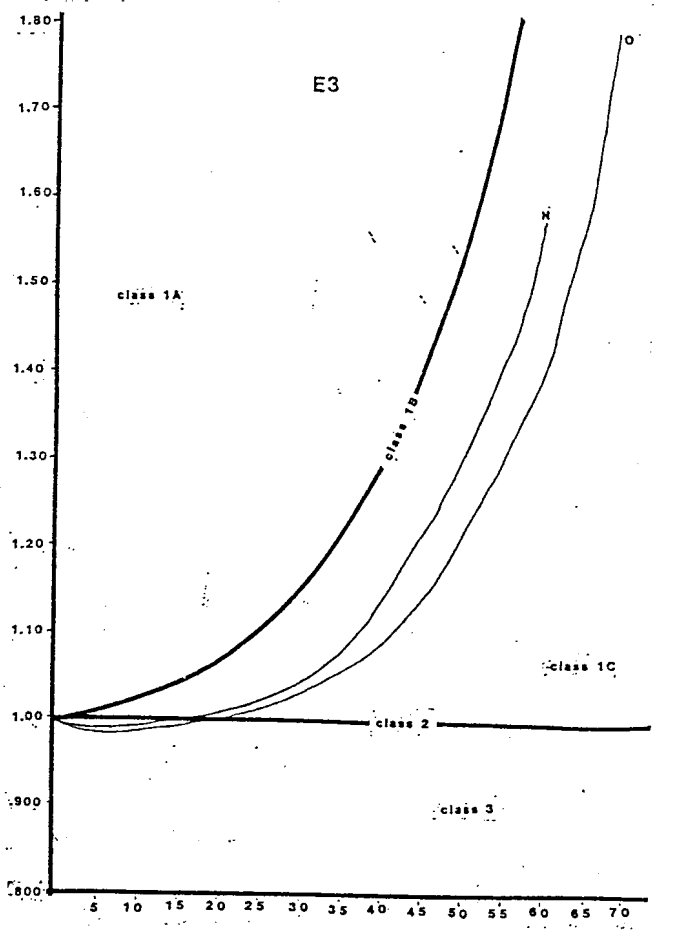

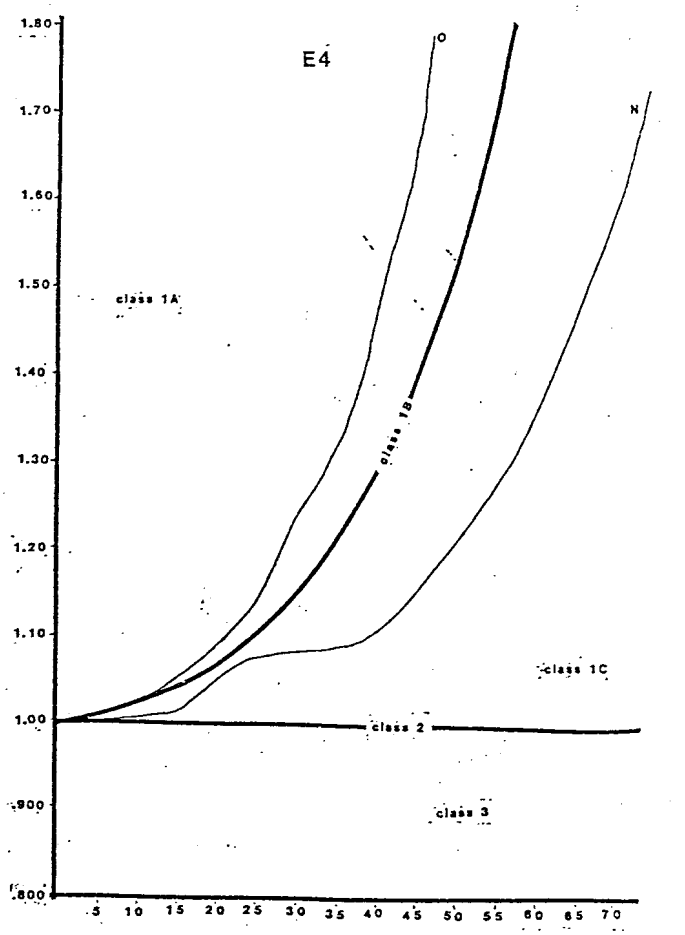

Figs. 18 a,b,c,d: T'_{α} graphs for fold E. "N" indicates normal limb, "O" indicates overturned limb.

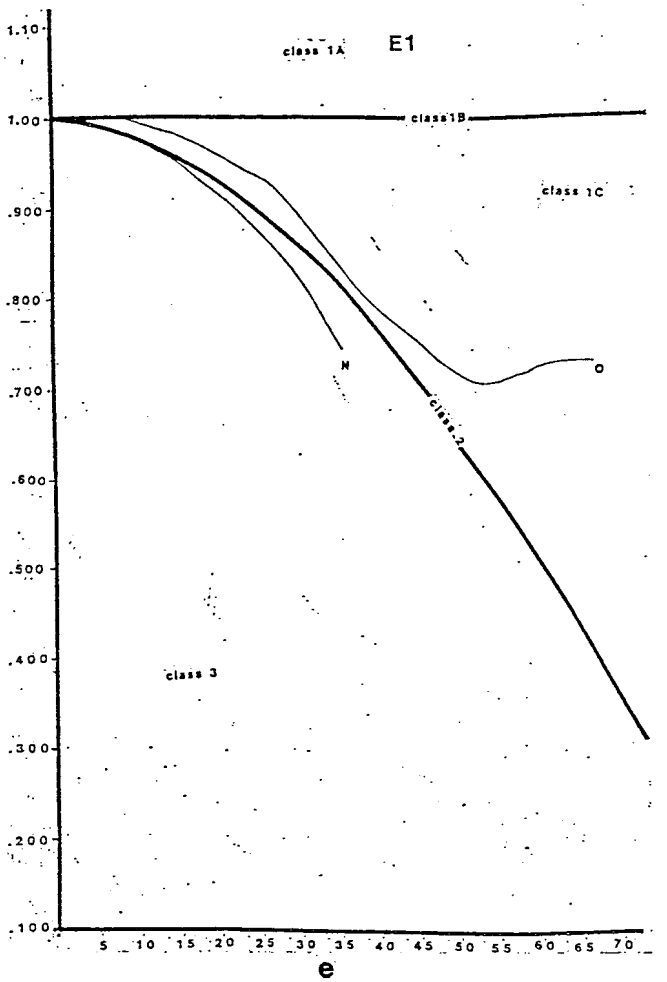

e

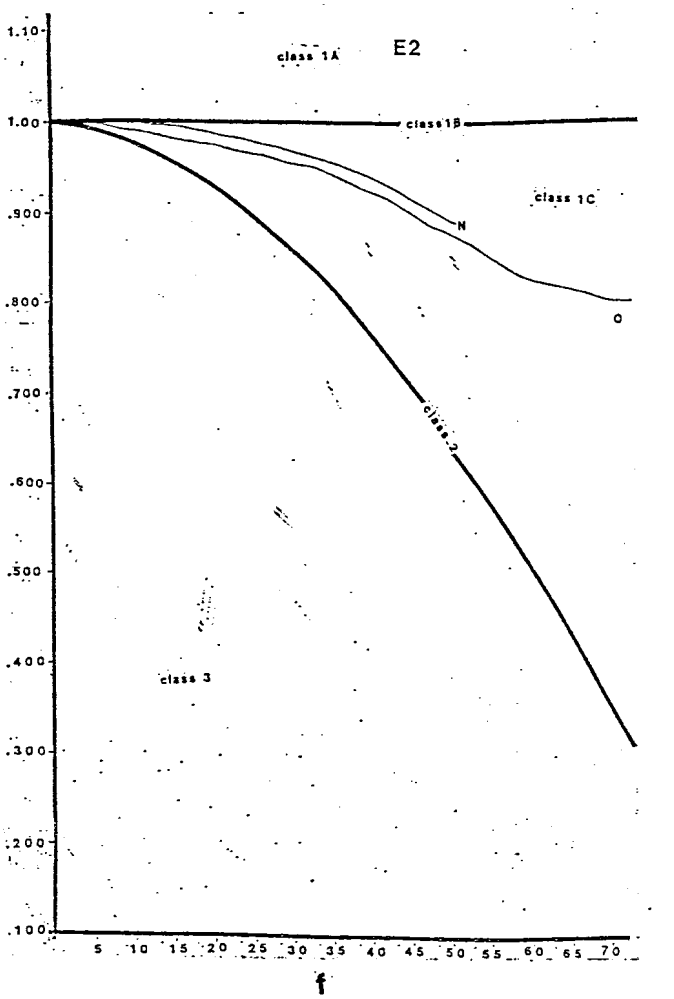

f

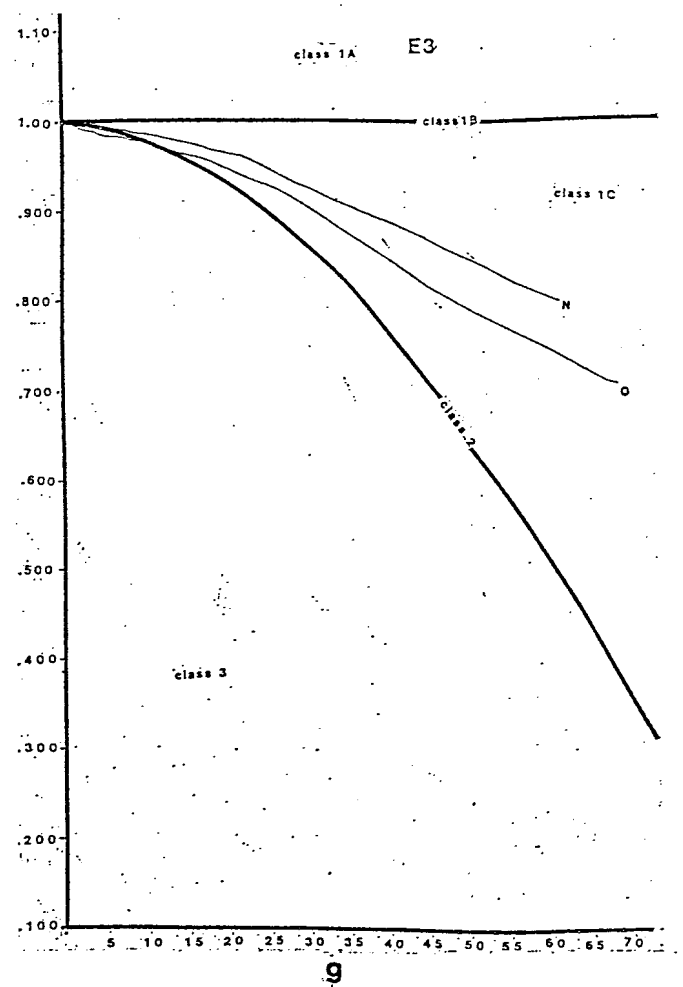

g

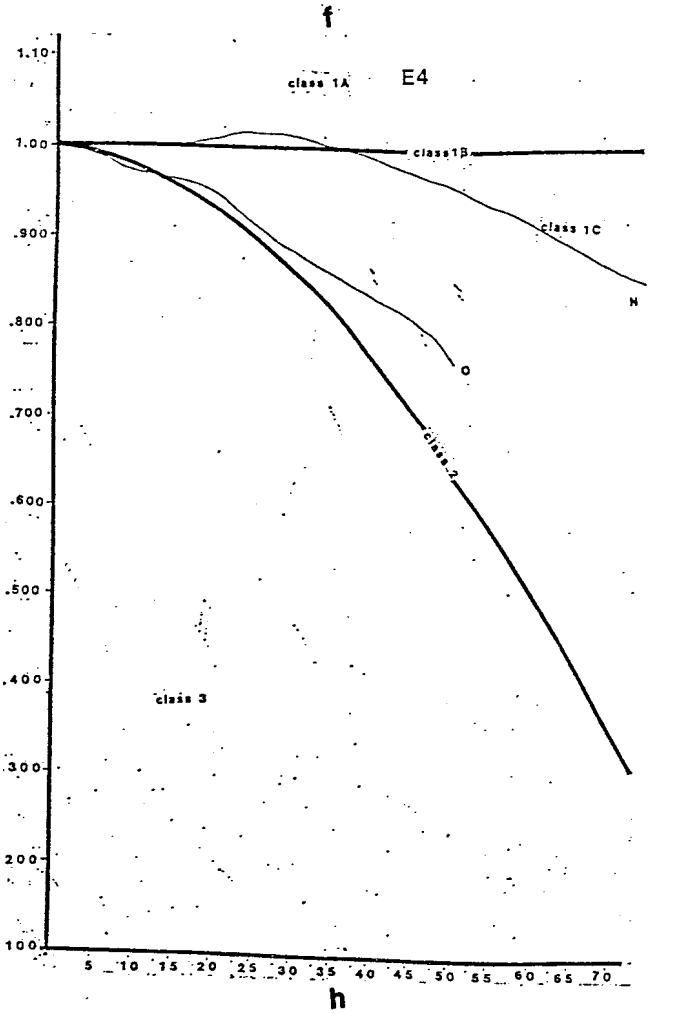

h

Figs. 18 e,f,g,h: t'_α graphs for fold E.

further in the core of the fold than in the outer layers. Referring to Table 1, which summarizes the results of the graphing study, one can see that for the values derived from t'_α graphs, the overturned limb of D1 plotted in the region of 10% flattening. The overturned limb of D3, however, plotted in the region of 80% flattening. The T'_α graphs reflected the same trend. The overturned limb of D1 fell in the class 1A field very close to the Class 1B curve. The overturned limb of D3, in contrast, plotted in the region of 70% flattening.

The trend toward an increasingly similar geometry within the inner core of fold D reflects greater shape modification due to the space limitations in the arc as the fold tightened. In the outer layers, the bulbous hinge areas represent collapse of the "saddle" structures formed by lift off of the layers during flexural slip (Fig. 19), (Profile 2: E). These hinge areas were also infilled by precipitated calcite and fine grained clay material flowing from the limbs of the fold where the flattening occurred. The intense axial planar cleavage seen only in the hinge zones of these outer layers indicate accommodation of the flattening also (Profile 2: F). The cleavage surfaces acted as conduits for transport of material, acting to thicken the hinge relative to its width.

The bulbous collapse features and the greater intensity of axial planar cleavage are not seen in the hinges of the inner layers of the fold, however. In contrast, the flattening mechanisms acting on the fold were accommodated by internal strain

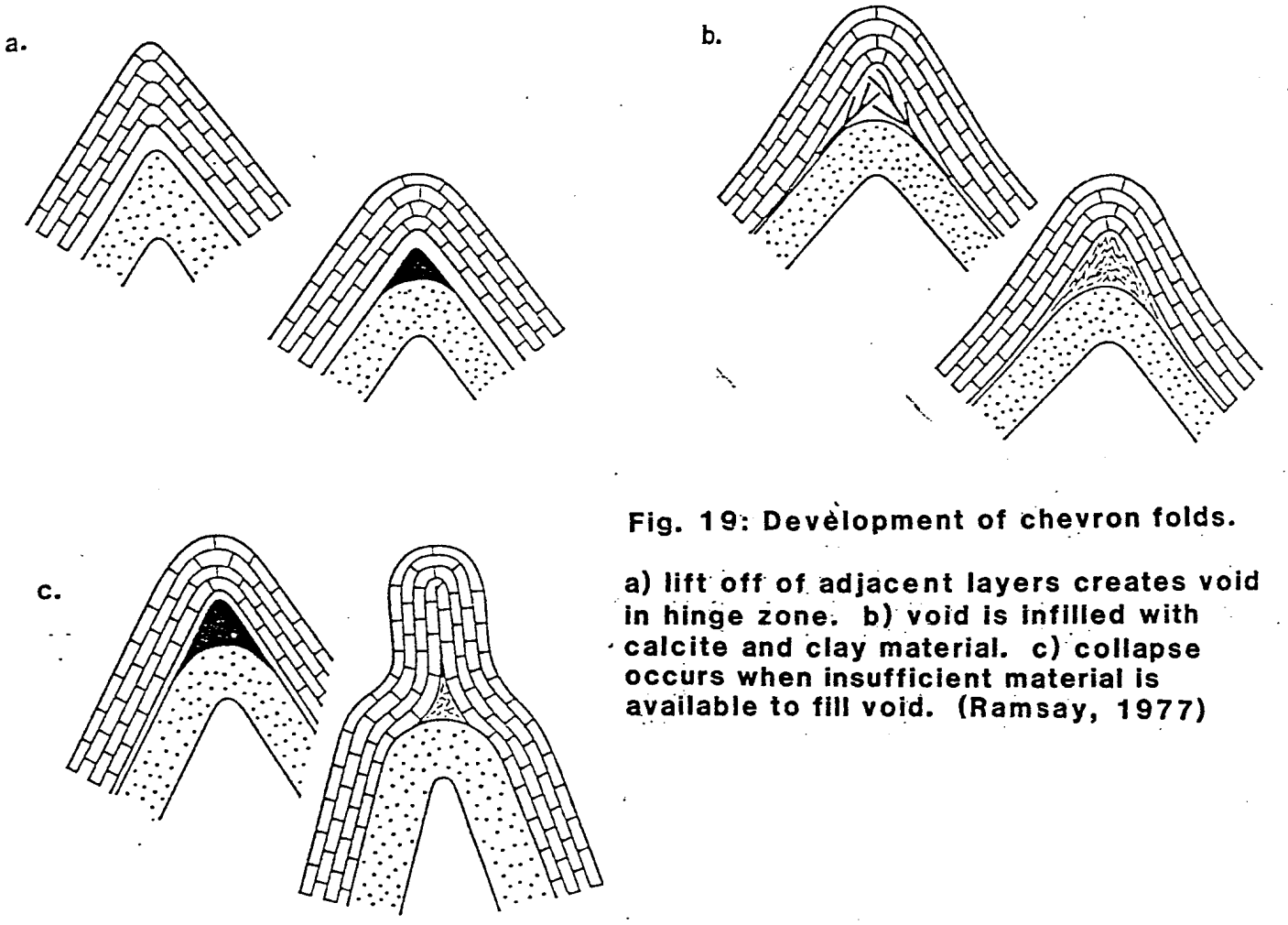

Fig. 19: Development of chevron folds.

a) lift off of adjacent layers creates void in hinge zone. b) void is infilled with calcite and clay material. c) collapse occurs when insufficient material is available to fill void. (Ramsay, 1977)

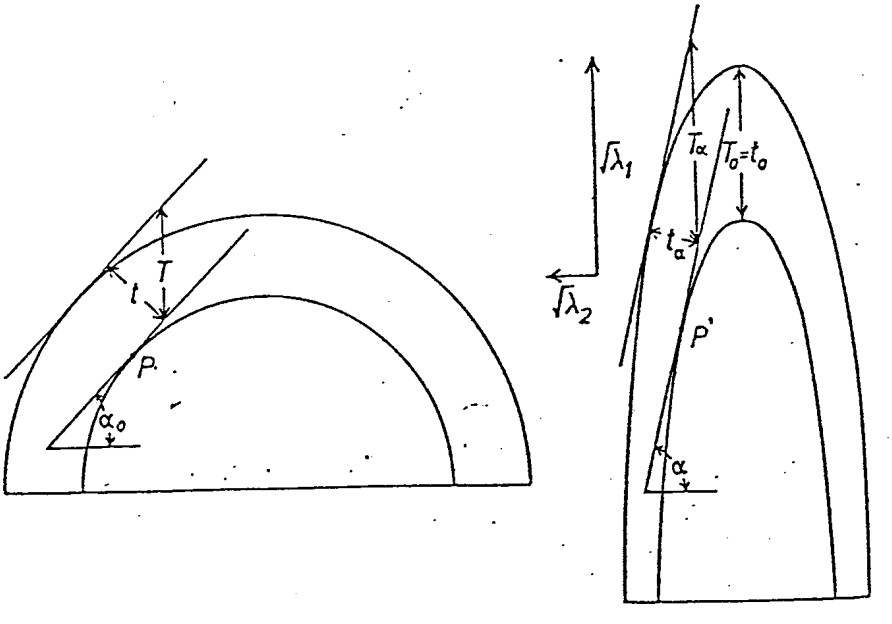

Fig. 20: Modification of the shape of a class 1B (parallel) fold by inhomogeneous strain. (Ramsay, 1967)

within the layers which thinned the limbs and thickened the hinge area, producing the more similar geometry in these inner layers. Also, flattening was probably accommodated here by the creation of calcite-filled thrust faults which were observed in the core of fold D. These faults displace bedding by several centimeters (photo 5), (Profile 2: G) These faults also deflect cleavage surfaces, providing a relative timing relation between fold flattening and development of the cleavage surfaces, which will be discussed below (Fig. 21a,b).

Another consistent trend is the increased amount of flattening exhibited in the overturned limbs compared to the normal limbs. In the outer layers of fold D, the amount of flattening in the overturned limb is less than that in the normal limb. Further in the core of the fold, however, the amount of flattening in the overturned limb is larger than that of the normal limb. Referring again to table 1, the normal limb of D1 plots in the 30% flattening region, while the overturned limb of D1 reflects only 10% flattening. In D3, however, the flattening in the overturned limb increases to 80%, while that of the normal limb is only 75%. One can see the same result for the values derived from the T'_{α} graphs.

The T'_{α} and t'_{α} graphs for the layers of fold E did not show a distinctive trend toward increased flattening in the inner core as did fold D (Figs. 23, 24). The t'_{α} and T'_{α} graphs for the normal limb of E1 through E4 show a decreasing flattening toward the inner core of the fold. In the normal limb E1 plots as a

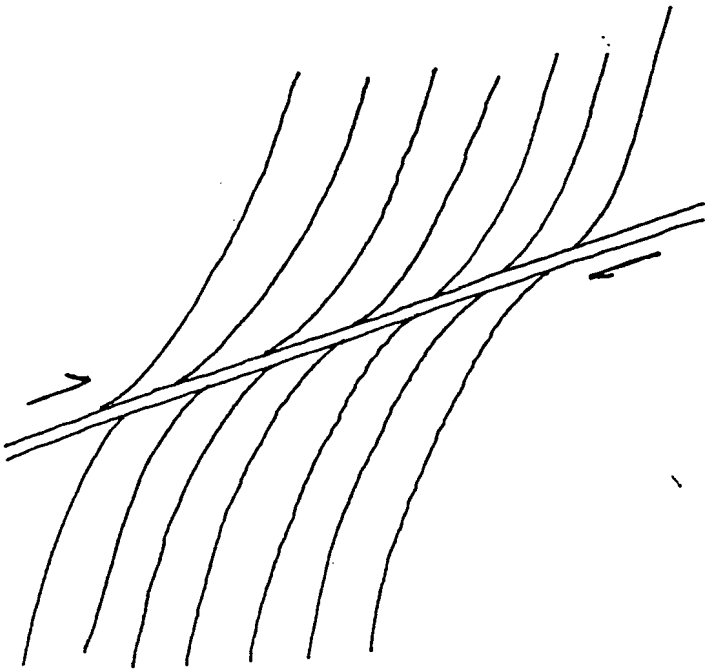

Fig. 21a: Diagram depicting "drag" of cleavage along slip surface.

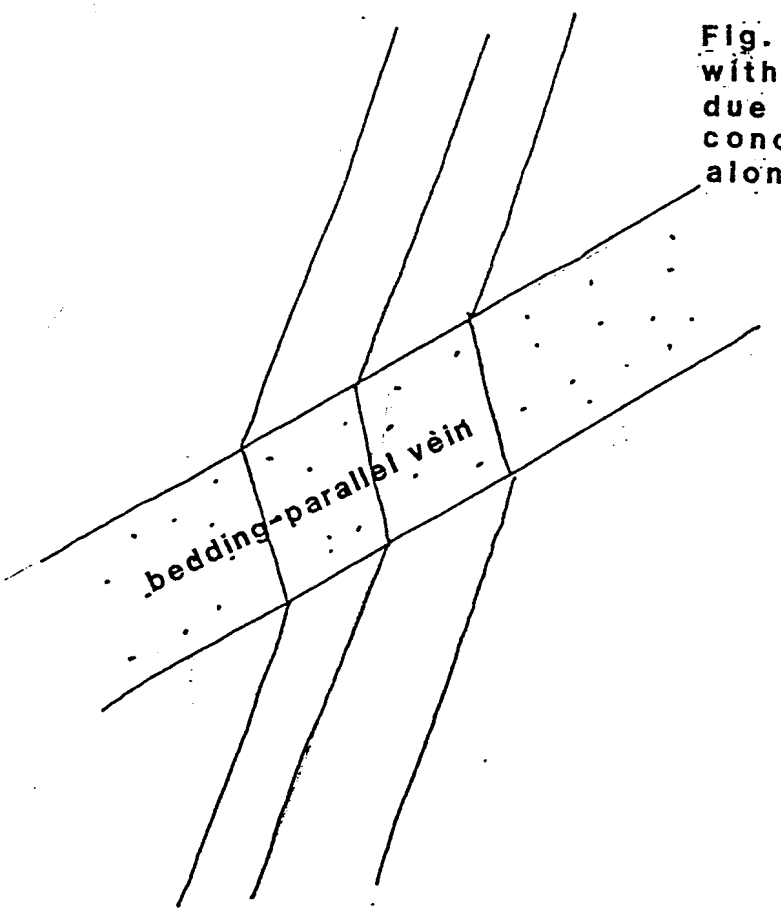

Fig. 21b: Deflection of cleavage within a bedding-parallel vein due to cleavage formation concurrent with, or after, motion along surface.

class 3 fold in both the t'_{α} and T'_{α} graphs. The normal limb of E2 then plots in the class 1C field in the region of 20% flattening in the T'_{α} graph. In the t'_{α} graph, the normal limb of E2 plots in the region of 35% flattening. The normal limb of E4 plots in the class 1A field in the T'_{α} graph, while in the t'_{α} graph, the normal limb of E4 falls along the class 1B line. It diverges to 25% flattening at an apparent dip of 30 .

Layers E1 through E4 for the overturned limb of fold E all plotted in the class 1C field in both the T'_{α} and t'_{α} graphs. The t'_{α} and T'_{α} graphs for the overturned limb first show a decrease in flattening from E1 to E2. There is then an increase in flattening from E2 to E4. (Table 1)

Because the normal limb of E1 is the only limb in this area of folding to plot in the class 3 field, it is possible that errors were made in tracing the curvature of E1 when the fold profile was constructed. This area of the fold contains an array of calcite veins incorporated in the hinge collapse structure which made it difficult to follow the fold surface continuously around the hinge zone (Profile 2: H). This possible distortion of the true shape of E1 could also have caused the break in trend toward increased flattening further in the core of the fold which was observed in the t'_{α} and T'_{α} graphs for the overturned limb. The fact that the overturned limb of fold E reflects the same larger amounts of flattening relative to the normal limb in every layer but E1 further indicates that errors were made in tracing the representative shape of E1. It can not explain, however, the

distinctive trend toward decreased flattening in the inner core observed in both the t'_{α} and T'_{α} graphs for the normal limb.

The analysis of the fold geometry of the southern area reveals a class 1B chevron geometry modified to that of class 1C - class 2. This geometry indicates buckling accommodated by flexural slip is a probable mechanism of folding (Ramsay, 1974). An increase in strain was found toward the inner core of fold D. The same was revealed in the t'_{α} and T'_{α} graphs for the overturned limb of fold E, but the opposite was found in the t'_{α} and T'_{α} graphs for the layers of the normal limb of this fold. Mechanisms of strain accommodation explain the results produced in fold D. No explanation is readily apparent for the conflicting data produced in the study of fold E.

The greater flattening consistently exhibited in the overturned limb of both fold D and fold E (the limb is common to both folds) can be explained by the orientation of the overturned limbs in space in relation to the probable orientation of the flattening direction (Fig. 22). The flattening modification can be assumed to have acted essentially perpendicular to the layers of the overturned limb. This flattening mechanism would have acted at an oblique angle to the normal limb of both folds. Therefore, greater flattening strain would be expected in this overturned limb common to both folds.

A geometric analysis was also completed for fold A in the northern section of folding. The t'_{α} diagrams produced for six layers of the fold demonstrated a trend different from that found

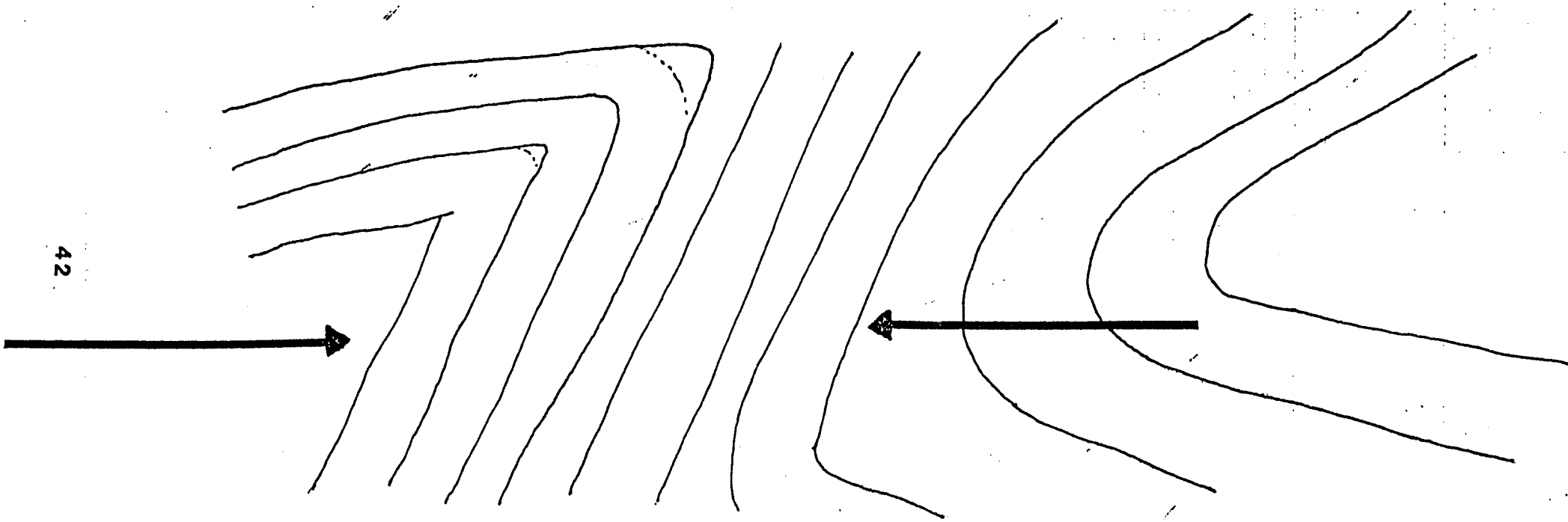

Fig. 22: Diagram depicting preferential flattening of overturned limb of folds D andE.

in the folds of the southern area. Here, there was an alternation between layers approximating a class 1B geometry with those exhibiting a class 1C geometry. In studying the graphs produced from these folded surfaces, it must be stated that the data taken is limited to measurements of tangent lines constructed up to only 40° of apparent dip. This limitation is due to the relative gentleness of the fold shape as compared to folds D and E, where measurements were derived up to 80° of apparent dip. Thus, the interpretation of the geometry (and amount of flattening) of the layers of fold A cannot be considered as precise as those made for the folds of the southern section.

Taking this into account, the alternating class 1B - class 2,3 geometry is still distinctive. The lower, outer layers of the fold (A1 and A2) plot in the class 1C region with about 50% flattening. A3, in contrast, follows the class 1B line. A4 also follows the class 1B line until it reaches an apparent dip of 25°, where it breaks away to plot in the region of approximately 25% flattening. A5 reflects a flattening of about 25% in its northwest dipping limb, while the southeast dipping limb more closely follows the class 2 line. This limb plots in the class 3 region. The innermost layer analyzed, A6, shows a pronounced difference between the geometries of the northwest- and southeast-dipping limbs. The southeast-dipping limb follows the class 1B line exactly. The northwest-dipping limb, however, plunges initially into the class 3 region and then crosses into the class 1C area, reflecting about 15% flattening. Since all other layers

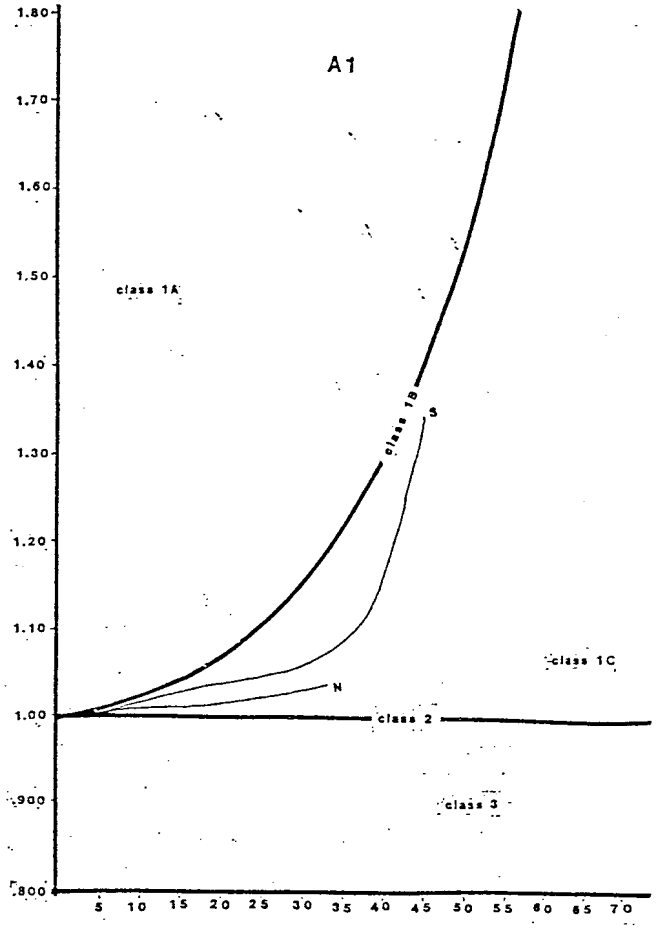

a

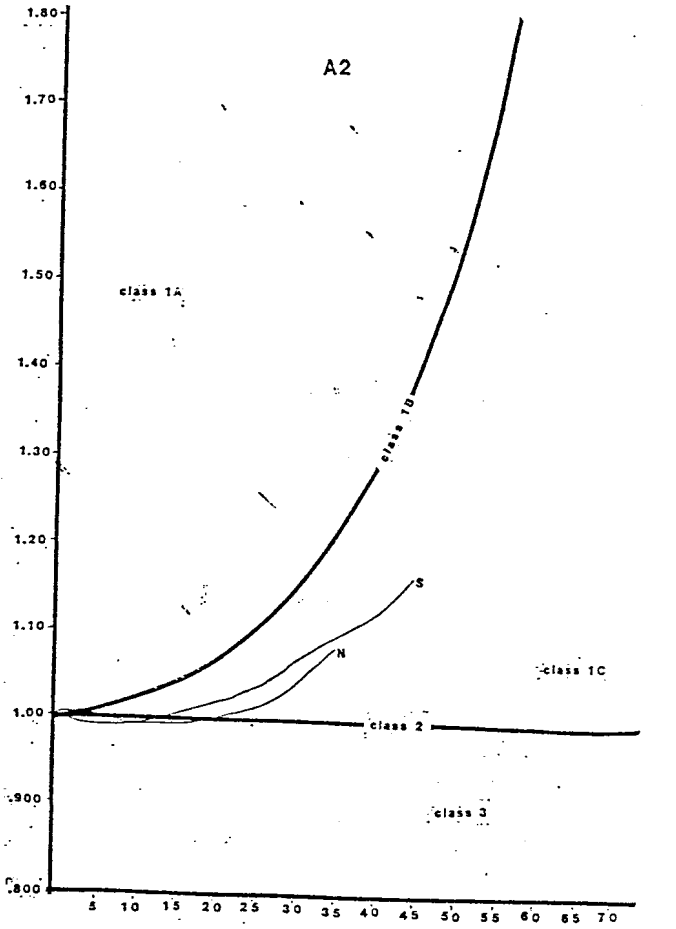

b

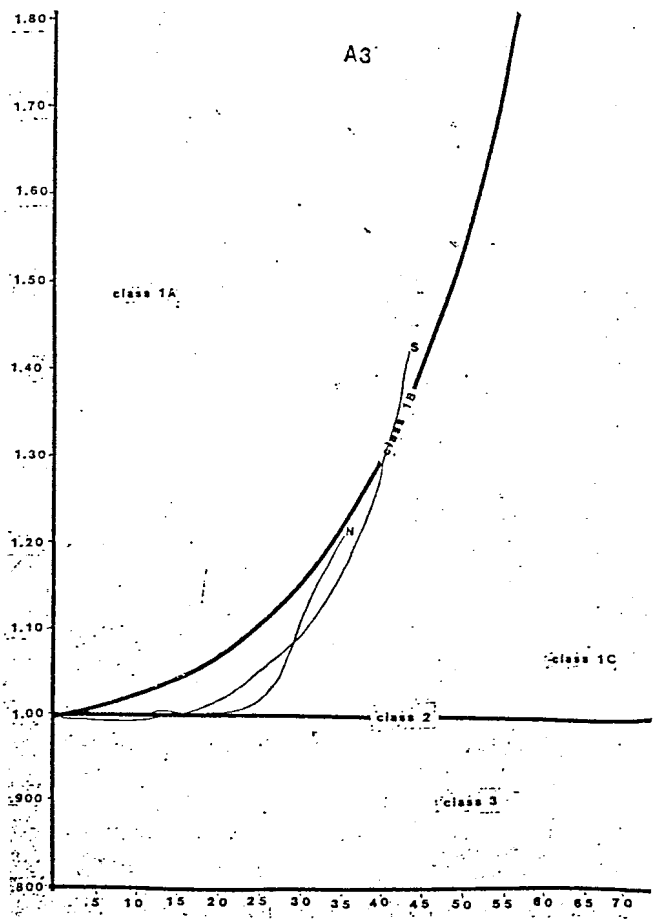

c

Figs. 23 a,b,c,d,e,f: T'₂ graphs for fold A. "S" indicates south dipping limb, "N" indicates north dipping limb.

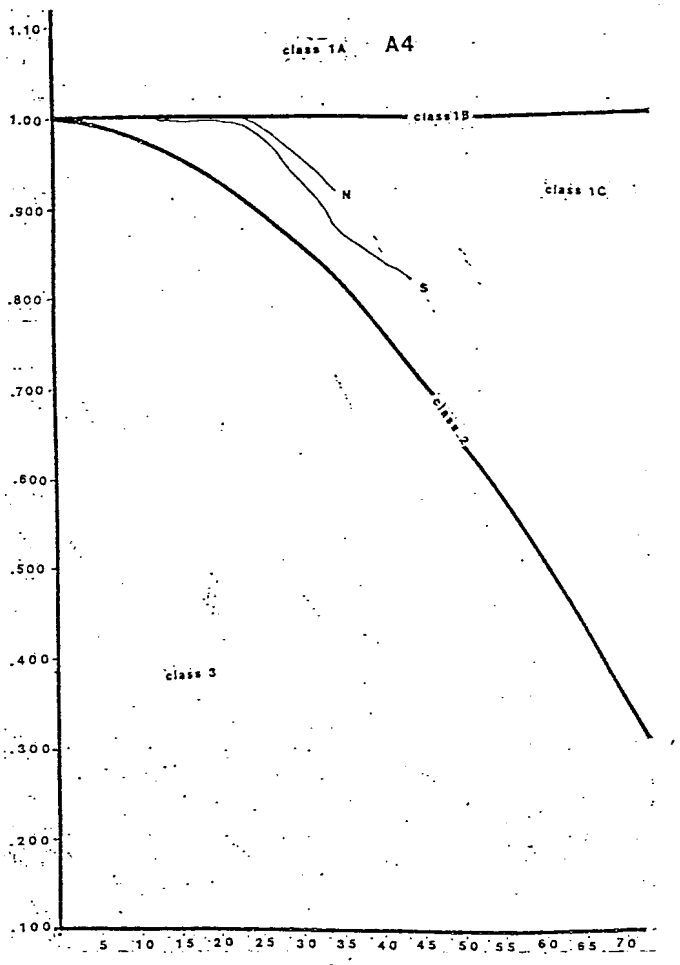
A4
class 1A
class1B
class 1C
N
S
class 2
class 3
1.10
1.00
.900
.800
.700
.600
.500
.400
.300
.200
.100
5 10 15 20 25 30 35 40 45 50 55 60 65 70

d

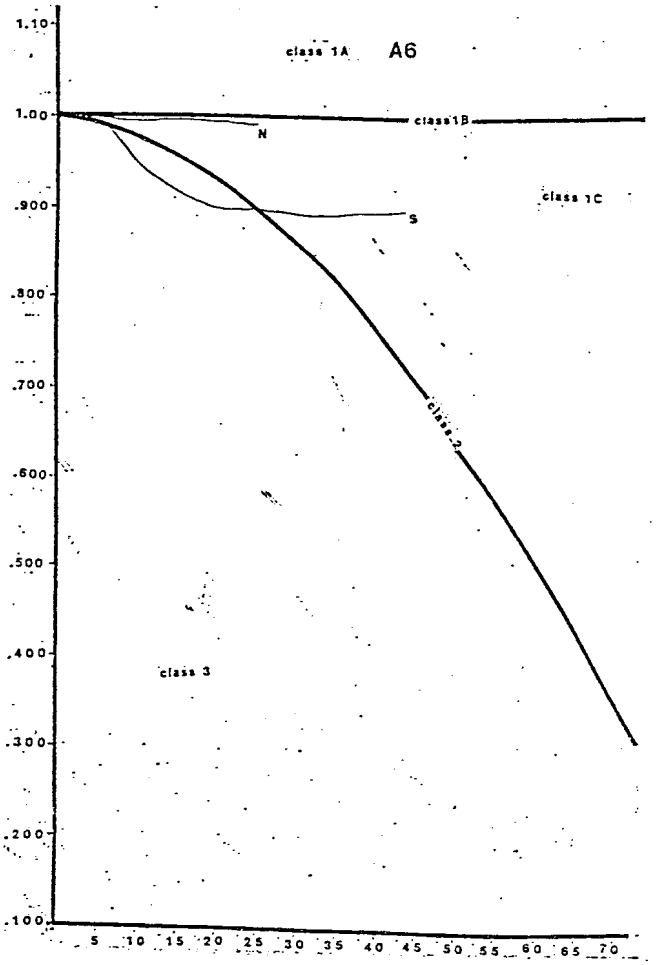
A6
class 1A
class1B
class 1C
N
S
class 2
class 3
1.10
1.00
.900
.800
.700
.600
.500
.400
.300
.200
.100
5 10 15 20 25 30 35 40 45 50 55 60 65 70

e

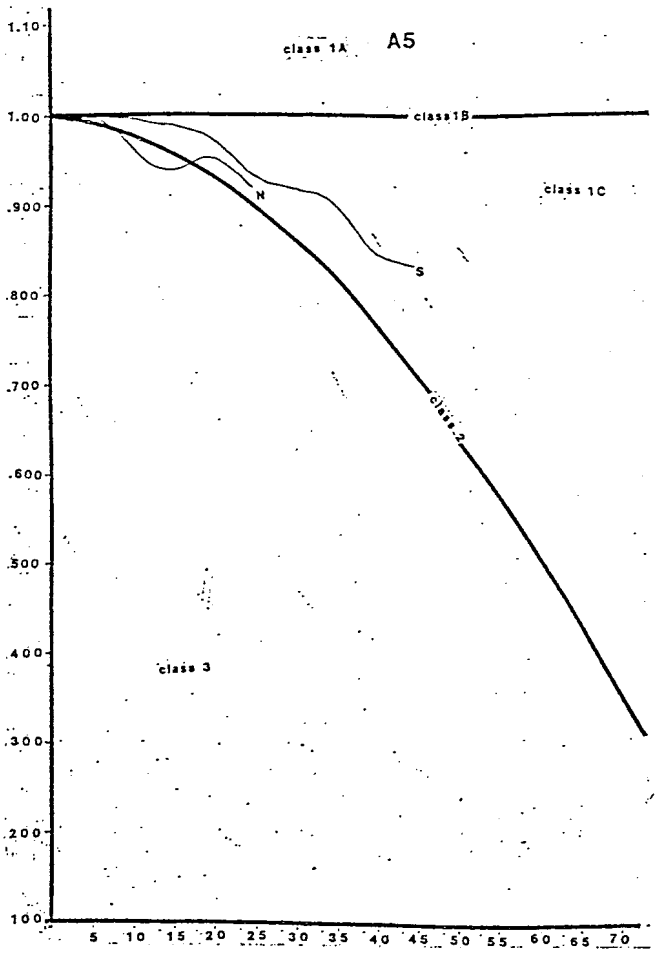
A5
class 1A
class1B
class 1C
N
S
class 2
class 3
1.10
1.00
.900
.800
.700
.600
.500
.400
.300
.200
100
5 10 15 20 25 30 35 40 45 50 55 60 65 70

f

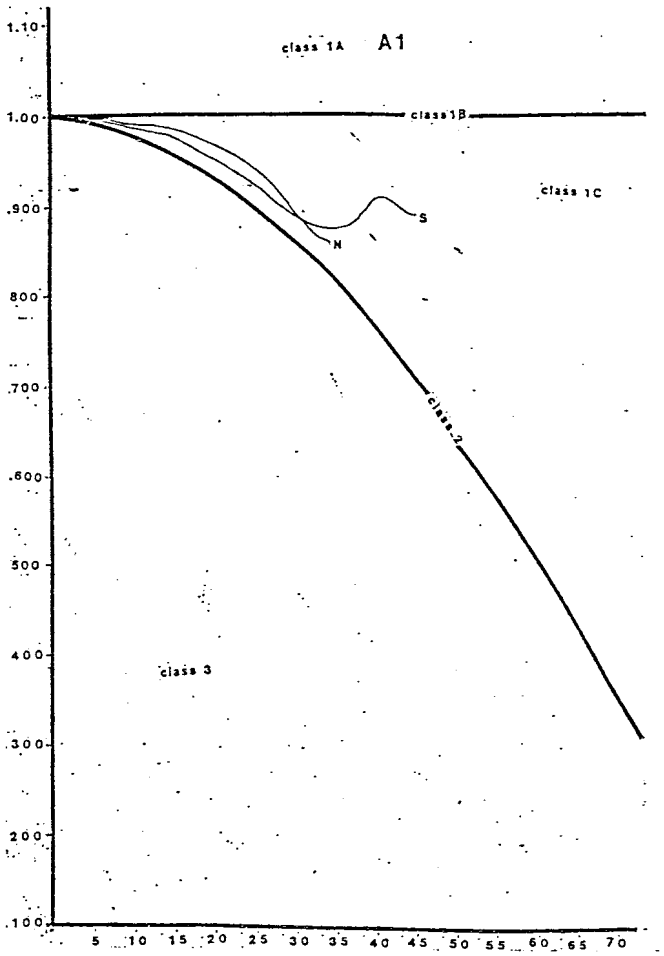

a

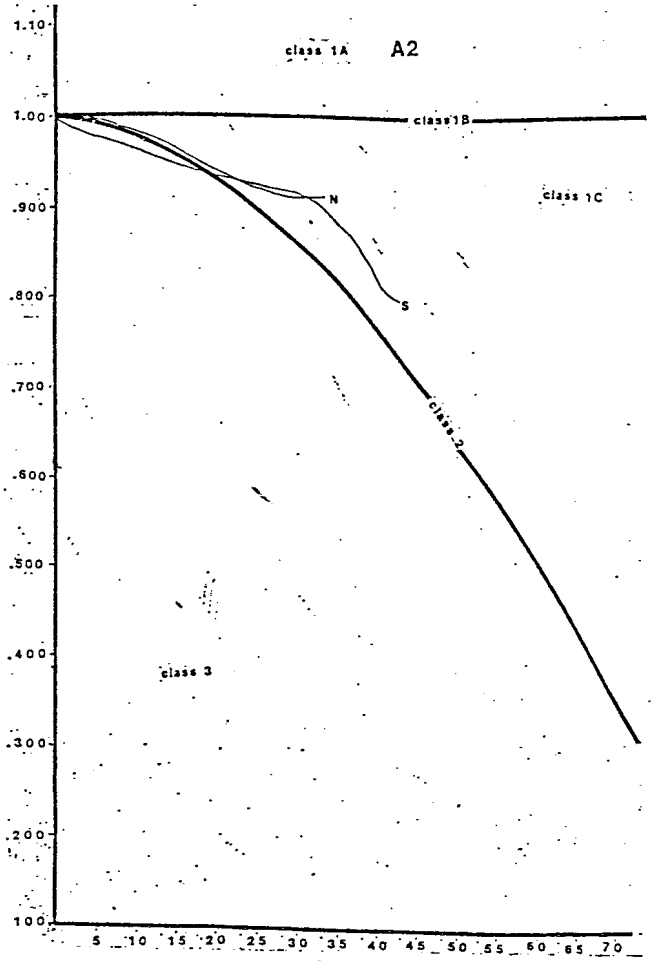

b

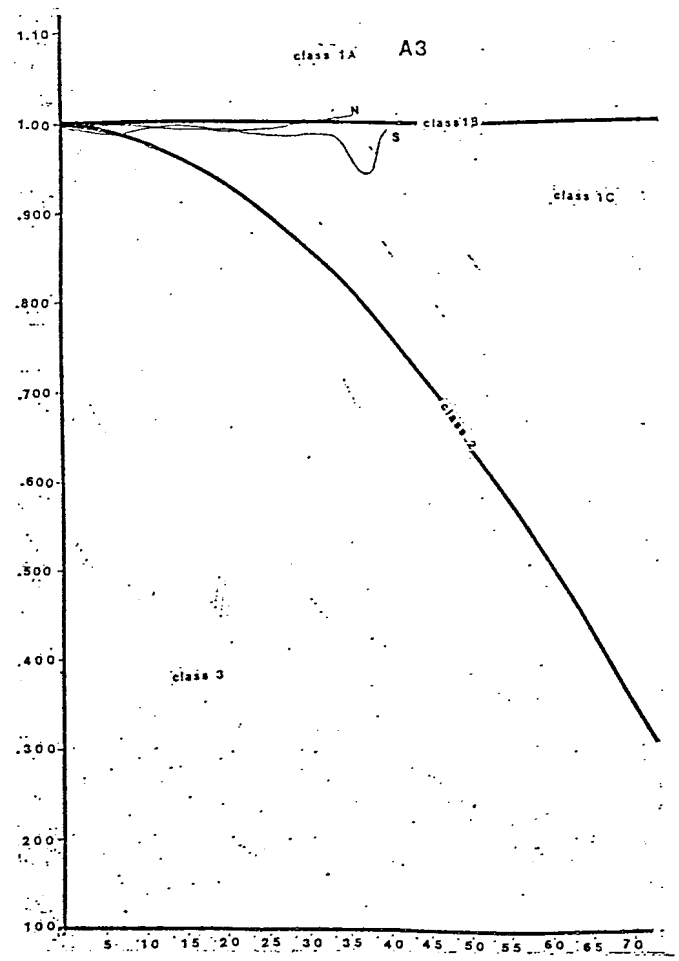

c

Figs. 24a,b,c,d,e,f: t'_α graphs for fold A.
'N' indicates north dipping limb,
'S' indicates south dipping limb.

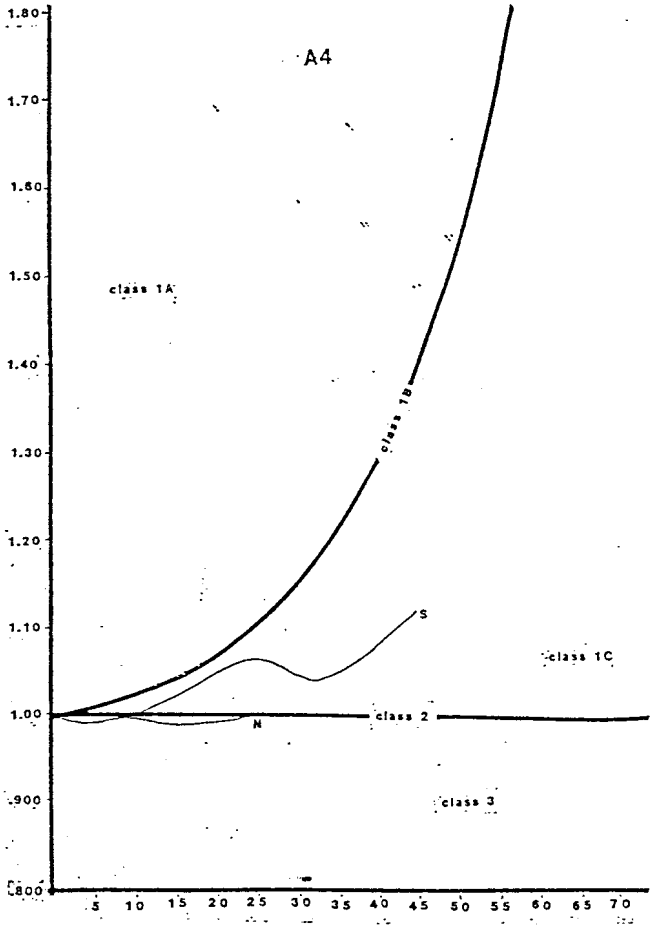
A4
1.80
1.70
1.60
1.50
1.40
1.30
1.20
1.10
1.00
.900
.800
class 1A
class 1B
class 1C
class 2
class 3
S
N
5 10 15 20 25 30 35 40 45 50 55 60 65 70

d

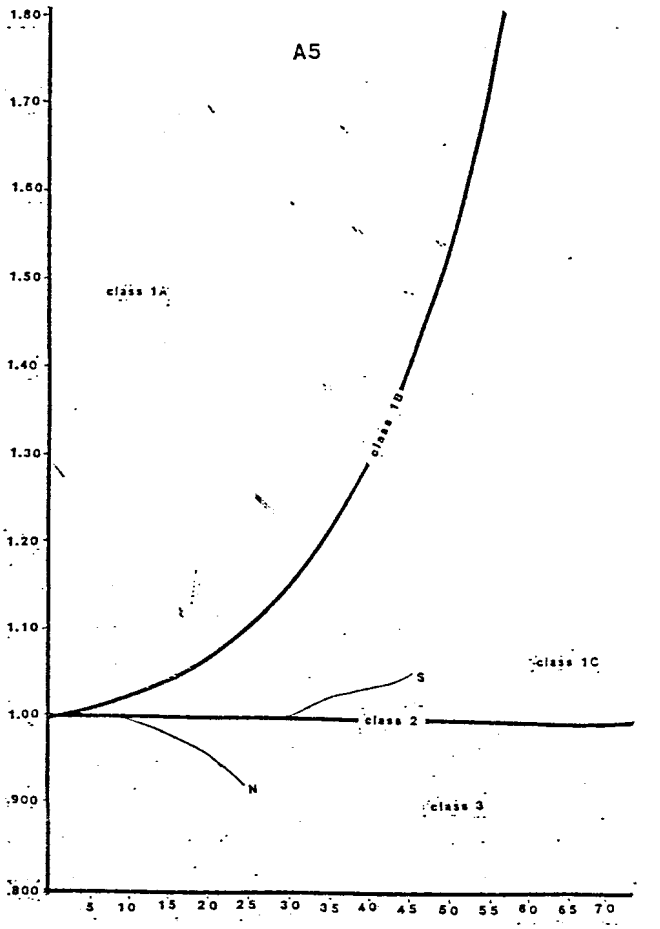
A5
1.80
1.70
1.60
1.50
1.40
1.30
1.20
1.10
1.00
.900
.800
class 1A
class 1B
class 1C
class 2
class 3
S
N
5 10 15 20 25 30 35 40 45 50 55 60 65 70

e

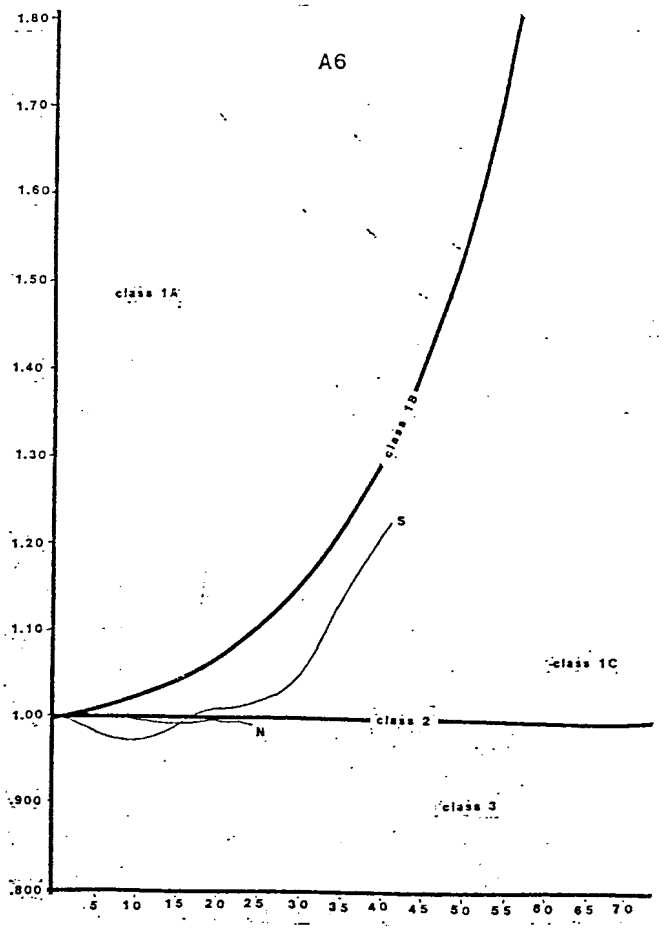
A6
1.80
1.70
1.60
1.50
1.40
1.30
1.20
1.10
1.00
.900
.800
class 1A
class 1B
class 1C
class 2
class 3
S
N
5 10 15 20 25 30 35 40 45 50 55 60 65 70

f

exhibit close correspondence between the two limbs, it is possible that this deviation in A6 is due to errors made in construction of the fold profile from the photographic mosaic. In this area of the fold, the bedding-parallel veins were not as visible in the photographs. Freehand estimation of fold curvature was thus used in part.

The alternation in class 1B/class 1C geometry reflects differences in mechanical behavior of the layers within fold A. The layers which have a class 1B geometry are more competent and controlled fold shape while constant thickness was maintained in them. The class 1C layers are more incompetent and were modified in shape to accommodate the geometry of the stiffer layers.

Both areas of folding show modification of an initial class 1B geometry to class 1C. A possible folding mechanism that produce this class 1B geometry is buckling accommodated by flexural slip resulting from buckling or fault propagation folding. Superimposed flattening occurred also on both areas of folds, either concurrent with the buckling-flexural slip process or after it. However, the greater shape modification of folds D and E reflects a greater flattening strain acting in this area. A possible explanation for this greater flattening strain will be presented below.

Kinematics of Thrusting and Folding

Bedding-Parallel Veins

Movement along bedding-parallel veins is an important element of the structural history of the rock unit studied. As stated previously, these veins consist of a buckled component and a planar component, and crosscotting relations indicate that they represent two separate slip events which occurred along the bedding parallel surfaces. The continuity of the buckled veins around the fold hinge zones indicates they were formed previous to any folding. Buckling then occurred, possibly concurrent with cleavage initiation. If these buckled components indeed formed previous to folding, the record of motion along them, existing as the stepped calcite lineations described above, would be in one general direction only. The evidence to be presented below indicates that this direction was to the northwest and that the hangingwall moved up to the northwest relative to the footwall. Thus, the buckled components are thrust fault surfaces.

The planar components of the bedding-parallel veins formed after the buckled components. They truncate the latter, and they do not exhibit the same degree of continuity around the fold hinge zones as do the buckled components. In many areas, they were observed to thin, and even die out, at the hinge zones of the folds. This suggests that these planar bedding-parallel veins may have formed during flexural slip. The focus of the kinematic analysis discussed below is to evaluate evidence indicating

whether a flexural slip mechanism played a role in fold development, and whether these planar components represent the surfaces over which this mechanism acted. This evidence includes a stereographic analysis of the orientation and movement sense exhibited by lineations measured at the outcrop and a discussion of other kinematic indicators found in the fold layers. Each concentration of lineations was examined to determine if the lineations of that population possessed pitches consistent with formation by flexural slip. A pitch of relatively high degree, around 90°, would suggest flexural slip. In the ideal model of flexural slip, this population of lineations would be expected to cluster around an orientation normal to the hinge line of the folds. The hinge line found for folds A, B, and C has an orientation of 12°, 238°. Therefore, one would look for a concentration of lineations oriented around 328° in order to suggest formation by flexural slip. One would also expect the step direction of these lineations to indicate motion from the inflection point of the fold toward the hinge zone on each limb of a fold (Fig. 8). In order to evaluate the hypothesis, the orientation and sense of slip associated with the lineations on the buckled components of the bedding-parallel veins must be compared with those on the planar components in the field. Regrettably, these distinctions were not recorded in the field. It is therefore necessary to make the assumption that any evidence from the measurements indicating flexural slip has its origin in the planar components. The structure of these surfaces and their

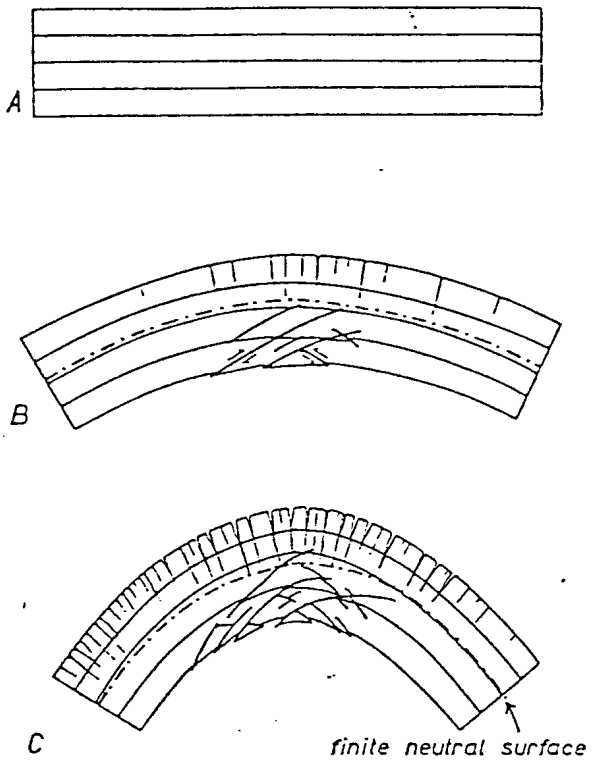

Fig. 25: Sequential deformation in layers folded by layer parallel compression (buckling). Note extension veins perpendicular to bedding in outer arcs and vein sets in inner core of fold. (Ramsay, 1967)

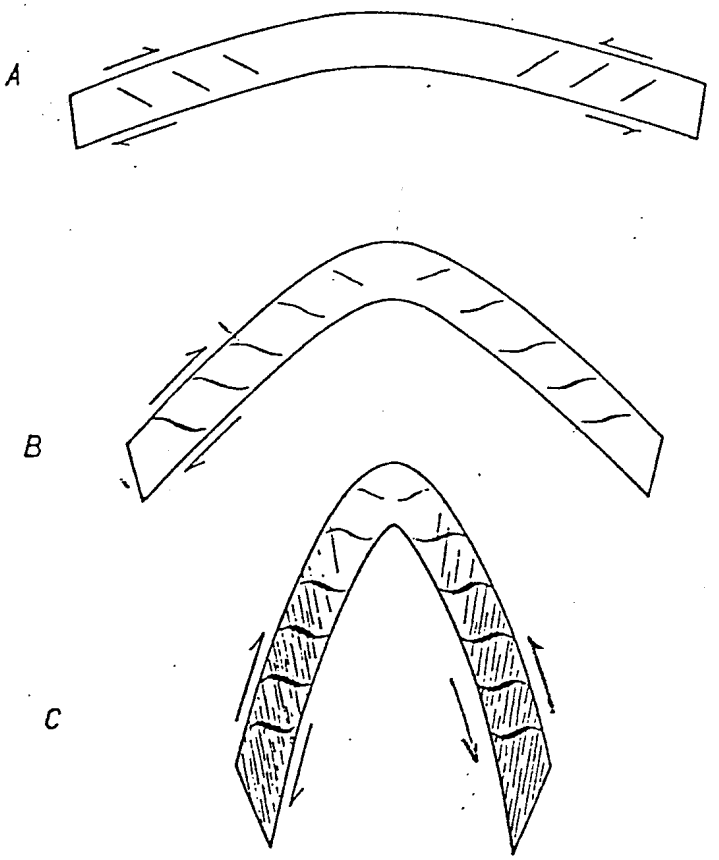

Fig. 26: Development of sigmoidal tension gashes. Arrows show sense of shear. (Ramsay, 1967)

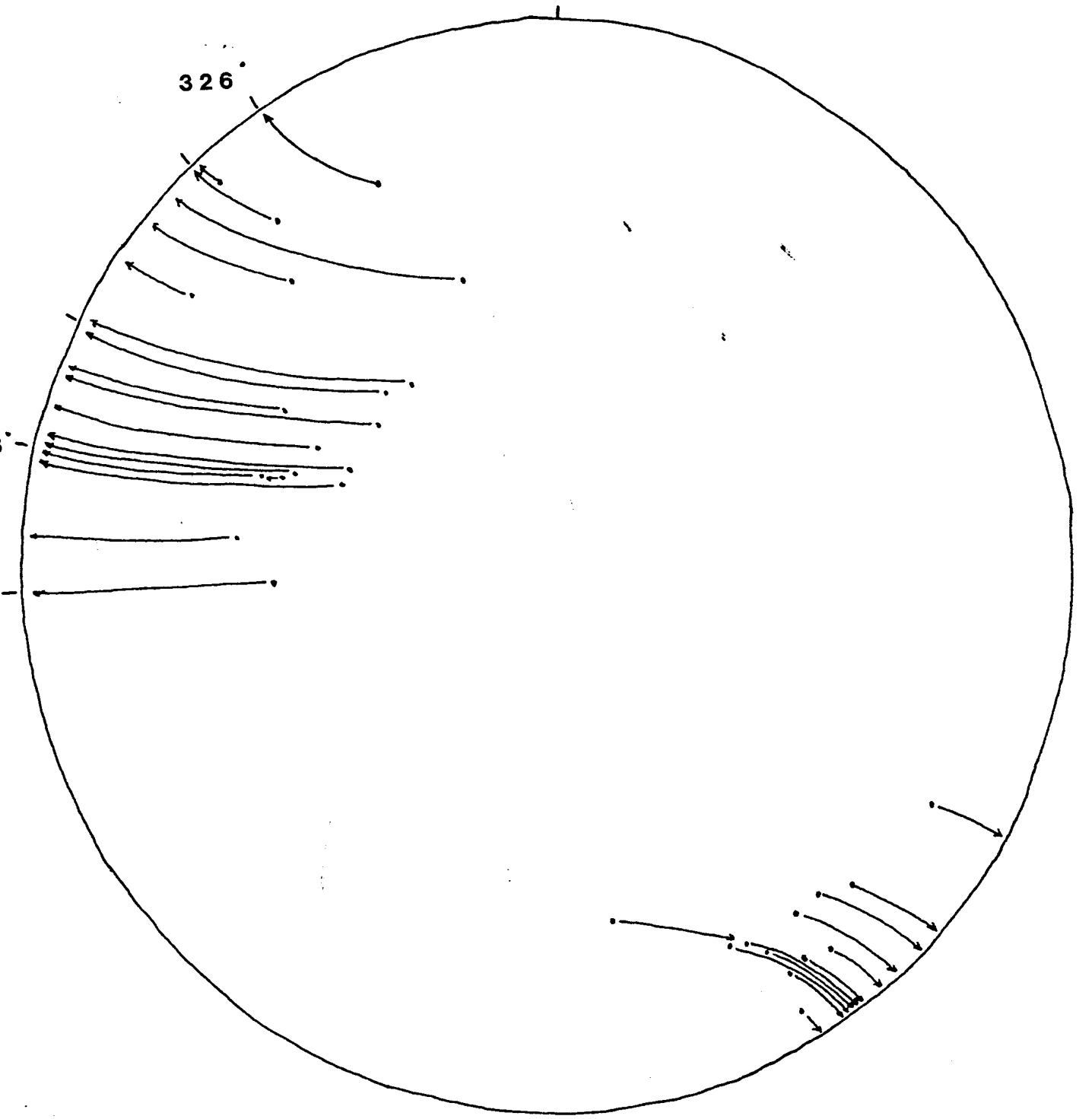

Fig. 27: Stereonet of slickenfiber lineations rotated along line of strike to a horizontal position. Orientations of two concentrations shown.

relation to the buckled components validates this assumption.

Stereographic analysis of 31 bedding-parallel calcite lineation orientation measurements was completed (Fig. 27). After all lineations were plotted and rotated around the line of strike of the surface back to a horizontal position to remove the effects of folding, a range of orientations from 267° to 326° was discovered. Within this range, two strong concentrations of data prevailed. One, containing five orientations, occurred at 283°. The other, containing seven lineations, occurred at the 326° endpoint of the range. Two smaller concentrations, each containing three lineations, occurred at 296° and 307°. The remaining lineations fell in a fairly even distribution throughout the range of the population between the major and minor concentrations discussed.

In order to single out a possible orientation for the flexural slip mechanism, the average pitch was calculated for each of the concentration points. Of the two major concentrations, it was found that the one at 326° had an average pitch of 82°, and the concentration at 283° had an average pitch of 80°. The two minor concentrations at 296° and 307° had average pitches of 76° and 71° respectively. Because the hinge line of the folds was found to lie at 12°, 238°, the concentration at 326° is most consistent with the orientation of lineations formed by flexural slip. This concentration lies 86° from the fold hinge line orientation and possesses the highest average pitch.

This population of lineations was also analyzed without

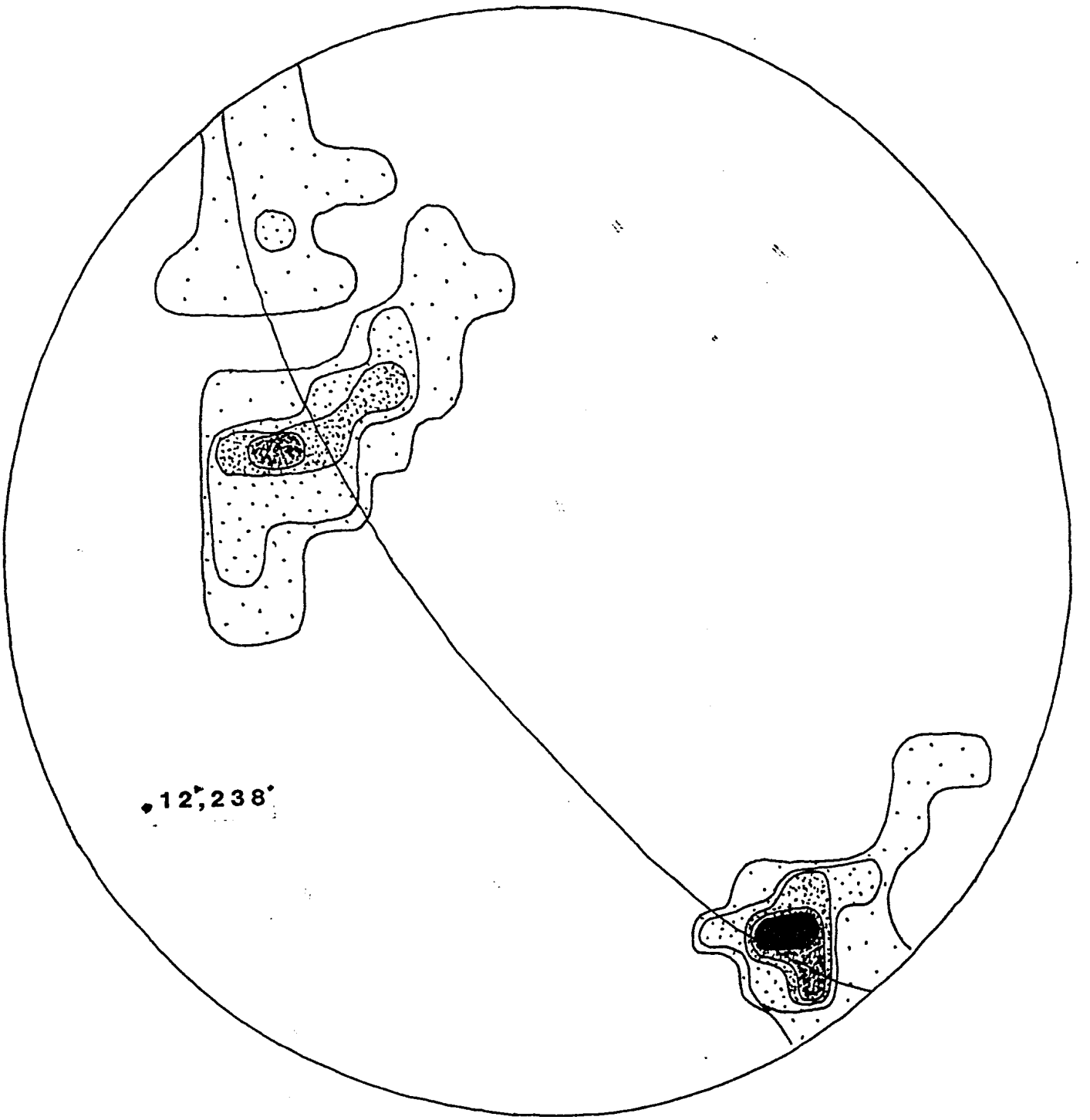

Fig. 28: Contoured density diagram of unrotated lineations. Areas of greatest density cluster around plane with a strike of 324°. Hinge line of folds indicated.

rotating the orientations back to horizontal. This was done to see if rotation had caused gross dispersion of the data points and hence, led to misrepresentation of a true concentration of points around certain orientations. A density diagram of the unrotated lineations was prepared (Fig. 28). The orientation of the hinge line of the folds is shown to demonstrate that the majority of lineations cluster around an orientation almost normal to the hinge line.

Analysis of the sense of motion assoicated with the lineated bedding-parallel veins provides evidence for both motion associated with thrust transport prior to folding and motion associated with the flexural-slip folding mechanism. Of the eight lineations measured where a directional sense could be identified with some certainty from the steps present, three contradicted formation by flexural slip. These lineations were measured on the north dipping limb of fold B near its hinge zone, and displayed a directional sense of the hangingwall down to the north. With this directional sense so close to the hinge area, they could not have been formed by flexural slip. Thus, they must represent the general northwest thrusting of hangingwall over footwall that occurred along the bedding-parallel veins. In the rotated plot, the orientation of these three lineations clustered at the 283° concentration, only 43° from the hinge line of the folds. This low angle to the fold hinge line is another indication that these lineations did not form by flexural slip.

One lineation indicated formation by flexural slip with

certainty. This lineation was measured near the hinge of fold A in its south-dipping limb. It indicated motion of the hangingwall down to the south. This motion is opposite to that expected for formation during the northwest thrusting interval that occurred prior to fold initiation. However, it is what is expected of formation by flexural slip. This lineation also had a pitch of 85° and occurred in the cluster of points at 326° in the unrotated plot. These are two more indications that this lineation formed by flexural slip.

The directional sense of the other four lineations was inconclusive. Due to their position on the limbs of the folds, the directional sense they displayed could have been formed by either the northwest thrusting or flexural slip.

Other Kinematic Indicators

Sigmoidal tension gash arrays that occur adjacent to bedding-parallel veins in the first and second tiers indicate shearing motion consistent with flexural-slip/flow folding. These arrays are not in contact with the bedding-parallel veins and are much smaller in scale than the more throughgoing extension veins in the southeast-dipping limb of fold A and in the second tier. These sigmoidal tension gashes are important indicators that flexural flow, the localized ductile shear which took place as the layers moved relative to each other to accommodate folding, occurred in association with flexural slip. In several areas in the first tier, arrays of gashes are present which possess a clockwise sense of rotation (Fig. 26), (Profile 1: H). These gash

arrays occur on the southeast-dipping limb of the fold. On the northwest-dipping limb, however, the tension gashes possess a counterclockwise sense of rotation (Fig. 26), (Profile 1: I). Thus, the gashes could not have formed prior to folding or they would all exhibit the same sense of shear. As they exist, these gash arrays display a rotational sense, or vergence, toward the hinge of the anticline. This sense of rotation would be expected for formation contemporaneous with folding accommodated by flexural-slip/flow.

Other vein sets within the area of folds A, B, and C can also be interpreted in the context of a flexural-slip folding mechanism. Here, the parallel array of extension veins in the hinge of fold A and the vein sets that occur in large numbers in the second tier conform to the model of fold development by buckling - flexural-slip presented by Ramsay (1967) (Fig. 25). In Ramsay's model, the outer arcs of the fold develop extension fractures roughly perpendicular to bedding and sets of fractures and thrust faults develop in the inner core, both to accommodate strain which builds as folding progresses. Each vein set surface accommodates this strain by movement along it, producing sets of thrust faults (Fig. 25). Of the calcite veins occurring at angles of about 60 to bedding-parallel surfaces in the second tier, slickenfiber lineations were observed on only two. One, oriented 338°, 89° NE, had lineations with a pitch of 60° W. The step direction indicated the hangingwall moved down to the northeast. Another lineation had an orientation of 322°, 87° SW and a pitch of

3° W. The step direction indicated that the hangingwall moved up, although its motion was almost strike slip in sense. Thus, on one surface normal faulting is indicated, and on the other, an almost purely strike slip motion is indicated. However, the scarcity of lineations on these surfaces did not allow analysis of the overall kinematics of these surfaces to be done.

One other set of slip surfaces exhibiting calcite fiber lineations was observed in the outcrop and will be discussed briefly. This set occurs in the first tier in the extreme northernmost portion of the outcrop (Profile 1: J). Several calcite veins at a high angle to bedding occur near the hinge zone of the gentle syncline in that area. One calcite vein, oriented 072°, 83° S, cuts almost entirely through the first tier, crosscutting bedding- parallel surfaces along its 8 meter length. This surface is displaced to the northwest by a bedding parallel surface approximately 1.5 meters from ground level. The pitch of the lineations observed on this high-angle vein indicates slip along it in a direction almost due east-west. This vein clearly has a history of formation separate from any vein discussed to this point, and most likely represents accommodation of compressive stresses acting relatively late in the structural history of the outcrop. It is still displaced by bedding parallel slip, though, indicating formation concurrent with flexural slip.

Timing Relations of Structures

The relative timing of the formation of the structures appearing in the rock unit provides important insights into the possible mechanisms which produced the deformation. The following discussion provides a concise formational history of the structures in this outcrop based upon the crosscutting relations observed and fold shape and kinematic evidence described above. It is hoped that this formational model can be used as a guide in seeking correlations between this outcrop and the structural processes occurring in, and acting on, the Saltville thrust sheet, of which this outcrop is a part. From these correlations, mechanisms of folding will be deduced.

Initial deformation of the Sevier Shale in this area is most probably represented by bedding-parallel veins associated with initial northwest directed movement. These surfaces are the buckled, laminated, components of the bedding-parallel veins. This statement is made based on the fact that the buckled veins are continuous around the entire curvature of the folds and therefore, must have been formed prior to folding. These originally planar veins were produced by a series of slip events that occurred between sheets of the country rock and represent movement of the hangingwall to the north relative to the footwall. Thus, these veins represent thrust fault surfaces initiated prior to folding.

The laminated nature of these veins suggest episodic periods of movement in which calcite was precipitated on the surfaces, followed by periods of rest. It is thought that the veins

containing fragments of country rock and which emanate from these buckled layers formed concurrently with them. They are definitely pre-folding structures, since they maintain near perpendicularity with the bedding-parallel veins consistently around the folds. They are not extension fractures which formed on the outer arcs of layers due to the folding process because they occur with the same frequency in the limbs as in the hinge area, whereas they would only be expected to form in the hinge area according to Ramsay's model (1967). More likely, these veins formed as the result of shear stress acting along the bedding-parallel surfaces during thrusting (Fig. 7).

Following the creation of the bedding-parallel veins, layer-parallel compression initiated the folding of these structures. The initial development of pressure solution cleavage, seen to maintain near verticality in the hinge zones of the folds while shallowing in dip in the limbs, was formed at this time. These cleavage surfaces were formed either concurrently with the buckling process, or perhaps prior to it.

Analysis of cleavage-fold relationships conducted by Gray (1981) on sandstones, limestones and calcareous mudstones of the Ordovician Mocassin Formation supports the conclusions drawn from evidence appearing in this outcrop of the Sevier Shale. Gray studied the Mocassin Formation in the Narrows thrust sheet in southwest Virginia, roughly 30 miles from this outcrop. The results of Gray's study have direct sifnificance for this outcrop of the Sevier Shale. Due to the proximity of the two areas of

study, their comparative positions within the fold and thrust belt, their lithological similarity, and the correlation in fold geometries between the two areas, it is reasonable to draw similar conclusions in the timing relations of cleavage initiation-folding-flattening mechanisms for this rock unit. From studies of the angular relationship between cleavage, fold axial surfaces and bedding in folds produced in the Narrows thrust sheet, Gray determined that cleavage was initiated prior to the folding history of the rock. His conclusions were based on the convergent fan nature of the cleavage to the axial surface and the orthogonal relationship of the cleavage to depositional bedding. The same relations are also seen in the outcrop studied in this paper.

From evidence provided by the same study, Gray (1981) derived particular mechanisms of folding which most likely acted on the Mocassin Formation and analyzed the timing of flattening relative to folding. Gray inferred a transition from buckling to flexural-slip/flow mechanisms during progressive fold development. Fold shape modification was thought to occur simultaneously with these mechanisms. Finally, cleavage was developed in "closely related, successive, noncoaxial strains during this protracted progressive deformation", with initiation prior to buckling (Gray, 1981).

The preservation of the orthogonal relationship between cleavage surfaces and bedding was observed in many areas of the outcrop. This relationship indicates the same pre-folding initiation of cleavage which Gray found in the Mocassin Formation.

The transition from buckling to flexural-slip/flow mechanisms thought to have occurred in the Mocassin Formation can also be seen in the Sevier Shale. As discussed above, the initial, continuous, components of the bedding parallel veins exhibit buckling. The planar components of the veins truncate the former, indicating formation after the buckling of the initial calcite surfaces. These planar veins are not continuous around the fold hinges, which is a structural characteristic of flexural slip folding. Also, the chevron geometry, with its saddle structures formed by lift off of the layers, is indicative of flexural-slip (Ramsay, 1974). Finally, the rotational sense of the tension gash arrays is yet another indication that a flexural-slip/flow shear mechanism occurred in the rock unit. Thus, the structural features exhibited in the outcrop support the conclusion that a buckling mechanism was followed by a flexural-slip/flow mechanism.

The class 1B and modified class 1C geometries consistently seen in this outcrop also correlate with those of the calcareous mudstone-argillaceous limestone units studied by Gray (1981). Although detailed studies like those performed by Gray were not done to determine the timing of flattening modification, it is reasonable to assume that the conclusion drawn by Gray can be applied here. That is, based on the striking similarities between the two areas, modification of the Class 1B geometry created by the buckling and flexural slip mechanisms occurred contemporaneously with folding.

Some evidence to support the claim that cleavage development

was closely related and concurrent with progressive deformation of the outcrop may be found in the faults observed in the core of fold D. As discussed above, these faults mostly likely were formed to accommodate flattening. Some cleavage was found to cut through the calcite infilling these faults, while other cleavage surfaces exhibited drag where they came in contact with the fault surface (Fig. 21 a,b), (Profile 2: I). These relations indicate a population of cleavage surfaces formed after movement along the faults, and a population formed either before or concurrently with movement along these faults. Formation of cleavage is related to the ongoing compression that caused flattening of the folds. Thus, cleavage development can be correlated with the flattening of the folds as well as occurring previous to any folding, as indicated by the fanning relation observed in the northern area.

Crosscutting relations between cleavage surfaces and other structures also support Gray's (1981) conclusion that cleavage was initiated prior to buckling and continued to develop throughout the structural history of the area. Cleavage seams were observed to cut through the buckled and planar calcite veins, in some places deflected within the veins or exhibiting drag near the contact with the outer edges of the veins. This indicates some cleavage formed currently with movement along these bedding parallel surfaces. Cleavage also cuts through the tension gash arrays, causing apparent displacement in some. This indicates these particular cleavage surfaces formed after the formation of these folding-related structures. As seen in thin section, the

cleavage also cuts through the clay-rich layers of the major thrust surfaces, causing truncation of folded bedding in the northern section. This stage of cleavage formation was concurrent with, or followed, movement along these thrust surfaces. Thus, there is evidence which indicates cleavage surfaces formed throughout the structural history of the rock unit.

The final structural relation to be discussed deals with the clay-rich thrust surfaces appearing in many areas of the outcrop, but studied in detail only in the northern section of folding. As discussed above, these surfaces occur near the hinge zone of the asymmetric syncline. The thrust surfaces follow bedding along the limb, then truncate bedding where they continue to cut up toward the northwest. The most obvious truncation can be seen in the southeast-dipping limb of fold A, approximately six meters above ground level in the first tier. These thrusts must have formed after the major portion of folding in the rock, for they truncate the folded bedding. Also indicative of a post-folding origin is the presence of the block of disconcordant bedding wedged between the bedding and the thrust surface in the hinge zone of fold A.

Other thrust surfaces which have a post-folding relation to the outcrop occur to the immediate south of fold D and within the core of fold D. The thrust to the south of fold D dips approximately 60° to the southeast and truncates and downwarps the southeast-dipping limb of fold D. This thrust surface and the one in the core of fold D are important because they may provide an explanation for the greater strain observed in folds D and E

compared to that in the northern folds.

Interpretation of Folding Mechanisms

With all structures and structural relations now fully discussed, an attempt can be made to correlate these features with the more regional deformational events occurring in, and acting on, the Saltville thrust sheet. Relating the structures at the outcrop scale will help to evaluate the contribution of the following folding mechanisms to the development of the observed structures.

1) fault propagation folding in a ramp-flat transport scenario (Fig. 4a).
2) simple shear strain within the thrust sheet during transport (Fig. 4b).
3) buckling due to layer parallel compression before thrust sheet transport (Fig. 4c).
4) buckling of the thrust sheet after transport and due to superimposed compressional strain.

The Southern Appalachians are thought to have formed by the progressive northwest transport of a series of sheets of thick sedimentary cover over the crystalline basement of the craton. This process, in which an initial master decollement surface separates the moving, deforming sedimentary sheets from the

Photo 5: Mineralized fault in core of fold D. Displacement of bedding-parallel veins can be seen.

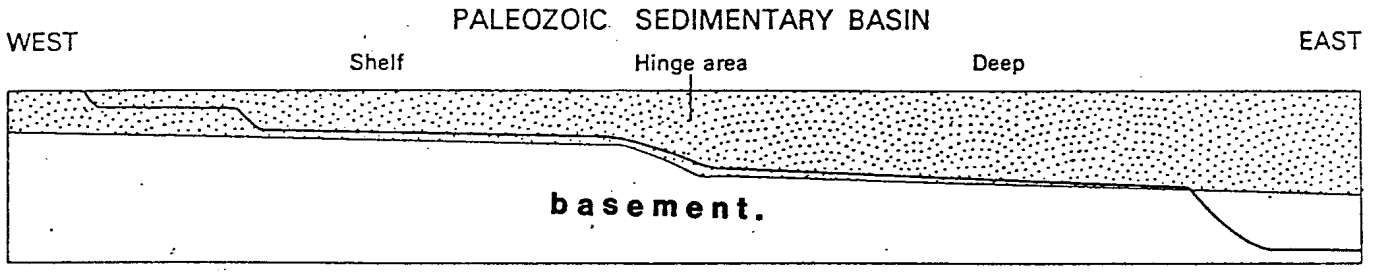

Fig. 29: Diagram depicting "thin skinned" style of deformation in fold and thrust belt. Sedimentary layers are translated from their original positions over the crystalline basement. (Harris and Miller, 1977)

relatively unaffected basement, is termed a "thin skinned" style of deformation (Harris and Milici, 1978) (Fig. 29). This initial master decollement then imbricates, creating a series of secondary thrust surfaces. The Saltville thrust is one of these surfaces.

There are two main theories as to the direction of progressive formation of these imbricate slices on the regional scale (Perry, 1978). One theory states that these secondary thrust surfaces begin near the craton and young toward the core of the orogenic belt, with successive stacking of thrust sheets within the hangingwall away from the craton (Fig. 30a). In the alternate, and more widely accepted, view, the earliest thrust surfaces form near the margin of the orogenic belt and successively younger thrust sheets move up from beneath previously emplaced sheets within the footwall toward the craton (Fig. 30b).

Studies of cleavage-fold-thrust relations in the Idaho-Utah-Wyoming thrust belt have indicated that cleavage was formed progressively toward the foreland as thrust sheets were emplaced over as yet undeformed layers (Mitra, 1985). This study has significance for the structural relationships found in the Sevier Shale. As discussed above, initial cleavage development is thought to have begun prior to folding of the bedding-parallel calcite veins. Thus, cleavage in the study area could have been formed by the overriding of the Pulaski thrust sheet on the layers contained within the yet undeformed Saltville thrust sheet. This emplacement of the Pulaski thrust sheet could have resulted in shear stresses which caused the initial, northwest-directed

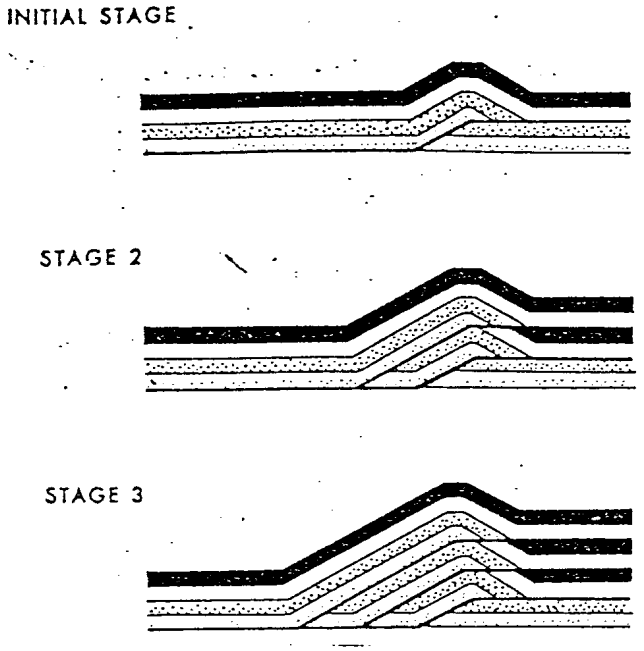

Fig. 30a: Diagram depicting hindward imbrication of thrust sheets (younging toward margin of continent). Sheets are stacked progressively toward margin. (Boyer and Elliott, 1966)

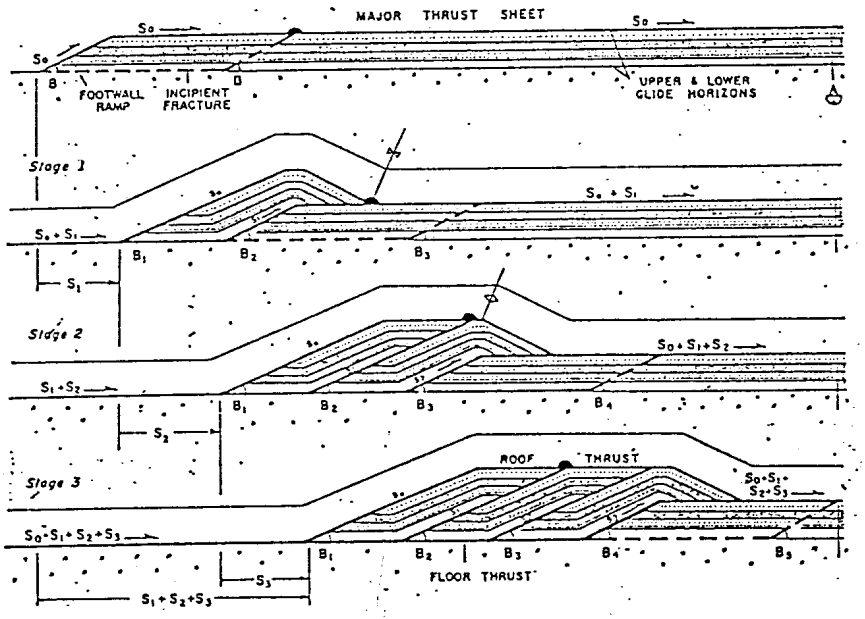

Fig. 30b: Diagram depicting thrust sheet emplacement progressively toward the craton (younging toward craton). (Boyer and Elliott, 1966)

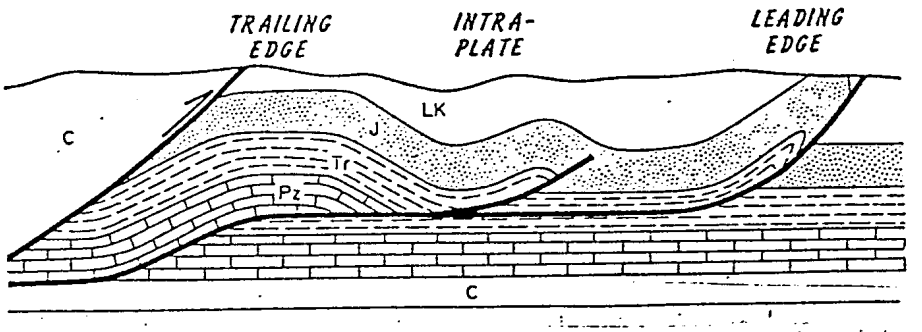

Fig. 31: Graphical presentation of Boyer's classification of the three main types of folds within a thrust sheet. (Boyer, 1986)

bedding-parallel slip along the thrust surfaces now represented by the buckled, bedding-parallel veins.

Alternatively, it is possible that the initial cleavage and bedding-parallel thrusting occurred during the initial stages of transport of the Saltville thrust sheet, before longitudinal compressive stresses were such that buckling of the calcite veins began.

The theory of thrust development younging toward the orogenic belt is supported by studies completed by Simon and Gray (1982). Their study involved folds formed in the Mocassin Formation contained within the Narrows thrust sheet. Their analysis of strain patterns found consistently greater strain exhibited in the southeast limbs than the northwest limbs of the folds in this area. Their conclusion was that this inhomogeneous deformation was associated with emplacement of the Saltville thrust sheet to the southeast. This conclusion suggests a marginward progression of thrust sheet emplacement.

Within the outcrop as a whole, an increase in strain from northwest to southeast is indicated by the tightening and more pronounced flattening of folds D and E in the southern area compared to folds A, B, and C in the north. A difference in strain magnitude within the folds, however, was only found within the overturned limb of folds D and E. The lack of consistently greater strain on the southeast limbs of folds in the outcrop does not support the conclusions of Simon and Gray (1982). However, the near central location of this outcrop within the Saltville

thrust sheet could be a possible reason why a strain pattern as seen by Simon and Gray in the Mocassin Formation is not observed here. The folds they studied were closer to the hanging wall of the Saltville thrust than this outcrop is to the Pulaski thrust. Therefore, thrust sheet emplacement younging toward the continental margin can not be ruled out, but is implausible.

The evidence provided by the fold geometry, cross-cutting relations, the relative position of the outcrop within the thrust sheet, and studies conducted on rock units in adjacent sheets indicates that folding of the Sevier Shale in this outcrop occurred during transport of the sheet. Boyer (1986) presents three types of folding which occur in a thrust sheet, including leading-edge, trailing-edge and intraplate folding (Fig. 31). This categorization is based on the relative position of the folds within the sheet and the characteristic geometries that these folds exhibit.

Leading-edge folds are generally sharp, overturned, truncated anticlines which propagate at fault tips. Trailing-edge folds are characterized by broad-topped anticlines created by the ramp-flat trajectory of thrust sheet emplacement. Intraplate folds consist of broad-bottomed synclines formed between the leading-edge and trailing-edge anticlinal folds. Smaller, imbricate faults and parallel folds of the kink band and chevron variety occur on the limbs of these broad-bottomed synclines to accommodate lateral shortening of the sheet (Boyer, 1986). The Bays Mountain Synclinorium, centered in the Saltville thrust sheet, can be

placed in this intraplate fold category. The structures examined in this study are considered to be the products of mechanisms operating in the thrust sheet which accommodated the lateral shortening associated with development of the Bays Mountain Synclinorium above a ramp-flat trajectory in the Saltville thrust sheet.

Simon and Gray (1982) provided a categorization of these smaller scale folds, faults, and their formational mechanisms which can be applied to the Sevier Shale. The gentle, symmetrical nature of the folds of the northern area, along with their modified class 1B geometry indicates they represent Group 1 folds with associated third order contraction faults. These contraction faults are characterized by displacements of less than 10 meters (Simon and Gray, 1982). The tight, overturned anticline-syncline pair to the south, with its chevron geometry, suggests that they are Group 2 folds associated with a third order contraction fault to the south.

Simon and Gray (1982) interpreted the folds of their study as caused by buckling due to layer-parallel compression rather than significant upwarping due to the subsurface ramp-flat geometry. The fold geometry, and the associations of the folds with small contraction faults accommodating flattening, in this outcrop of the Sevier Shale are similar to the features described by Simon and Gray, suggesting a similar origin. The gentle folds in the northern area, with their interlimb angles of approximately 100 , and alternating class 1B and 1C geometry are comparable to the

folds in the calcareous mudstones studied by Simon and Gray. They are characteristic products of the buckling - flexural slip mechanisms which Simon and Gray found for the Mocassin Formation folds. The clay-rich thrust surfaces, already proven to occur in the later stages of fold formation, accommodated strain which grew as the fold developed.

The tight, overturned nature of the folds of the southern area, and the throughgoing fracture in the axial surface of fold E are superficially similar to the fault propagation folding model presented by Suppe (1983). Thus, these folds might be thought to exist as the upper tip of a fault propagation fold created by a minor imbrication above a thrust ramp. It is more likely, however, that the distinctive geometry and strain particular to the folds of the southern area occurred from flattening strain induced by the smaller imbrication within the sheet rather than fault propagation folding. Possibly, the thrust surface truncating bedding in the south-dipping limb of fold D and the fractures within the cores of folds D and E represent the upper tip of this imbrication. This imbrication propagated up through the layering of the sheet as the folds formed. It then reached the folds after partial, or near completion of, fold development. This is indicated by the displacement and downwarping of folded bedding.

This chevron fold-fault association is comparable to relationships described by Simon and Gray involving Group 2 folds and third order faults. They describe these folds as produced in

close association with contraction faulting generated along detachment zones between the Mocassin Formation and underlying Middle Ordovician limestones. The thrust surface to the south of fold D may have been generated along the same kind of zone of weakness during thrust transport.

Conclusions

Analysis of fold geometry and the structural relations between folds, bedding-parallel slip surfaces, and cleavage in an outcrop of the Sevier Shale located in the Saltville thrust sheet indicate fold formation by buckling-flexural slip/flow mechanism. The classic profile forms, representing modified 1B geometries, in folds in the outcrop indicates buckling followed by flattening. The lift-off mechanism that created the chevron geometry in folds D and E, and the kinematic analysis of lineation orientations and strain patterns found in folds A, B, and C, indicate a flexural slip/flow mechanism acted to accommodate buckling of the layers. These mechanisms acted contemporaneously with thrust sheet transport over an underlying ramp-flat trajectory that produced the Bays Mountain Synclinorium. The folds of this outcrop formed due to the mechanisms acting to accommodate layer-parallel shortening within the thrust sheet as the Bays Mountain Synclinorium developed. Modification of the folds from that of the original class 1B geometry produced by the folding mechanisms

is thought to have occurred progressively during fold amplification. Thus, modification occurred during thrust transport as well.

The chevron geometry and tight overturned nature of the folds in the southern area of the outcrop differ significantly from the gentle folds of the north. These differences reflect an increase in strain in the southern area relative to the north. The differential strain may be related to the formation of a subsidiary imbricate thrust within the Saltville thrust sheet just to the south of the study area.

References

Boyer, Steven E., 1986, Styles of folding within thrust sheets; examples from the Appalachian and Rocky Mountains of the U.S.A. and Canada, Journal of Structural Geology, vol. 8, no. 3, pp. 325-337.

Boyer, Steven E., and David Elliott, 1982, Thrust systems: American Association of Petroleum Geologists Bulletin, vol. 66, pp. 1196-1230.

Gray, D. R., 1981a, Cleavage-fold relationships and their implications for transected folds: an example from south-west Virginia, U.S.A., Journal of Structural Geology, vol. 3 no. 3, pp. 265-277.

Harris, L. D., and R. L. Miller, 1977, Characteristics of thin-skinned style of deformation in the southern Appalachians and potential hydrocarbon traps, U.S. Geological Survey Prof. Paper 1018, 40 p.

Hunt, Charles B., 1967, Physiography of the United States: San Francisco, W. H. Freeman and Company, p. 9.

Marshak, Stephen, and Gautum Mitra, 1988, Basic Methods of Structural Geology: Prentice-Hall, Inc.

Mitra, G., and W. A. Yonkee, 1985, Relationship of spaced cleavage to folds and thrusts in the Idaho-Utah-Wyoming thrust belt, Journal of Structural Geology, vol. 7, pp. 361-373.

Perry, W. J Jr., 1978, Sequential deformation in the Central Appalachians, American Journal of Science, vol. 278, pp. 518-542.

Ramsay, J. G., 1967, Folding and Fracturing of Rock: New York, McGraw Hill Book Company, 567 p.

Ramsay, J. G., 1977, Development of Chevron folds, Bulletin of Geological Society of America, vol. 85, pp. 171-175.

Ramsay, J. G., Martin Gray, and Roy Kligfield, 1983, Role of shear in development of the Helvetic fold-thrust belt of Switzerland, Geology, vol. 11, pp. 439-442.

Shanmugan, Ganapathy, and Kenneth R. Walker, 1978, Tectonic Significance of distal turbidites in the Middle Ordovician Blockhouse and Lower Sevier Shale Formations in east Tennessee, American Journal of Science, vol. 278, pp. 551-578.

Simon, Robert I., and David R. Gray, 1982, Interrelations of mesoscopic structures and strain across a small regional fold, Virginia Appalachians, Journal of Structural Geology, vol. 4, no. 3, pp. 271-289.

Suppe, J., Principles of Structural Geology: New Jersey, Prentice Hall, Inc., p. 351.

Woodward, Nicolas B., ed., 1989, Geometry and Deformation Fabrics in the Central and Southern Appalachian Valley and Ridge and Blue Ridge, Field trip guide book T357.

Woodward, Nicolas B., ed., 1985, Valley and Ridge Thrust Belt: Balanced Structural Sections, Pennsylvania to Alabama, University of Tennessee Dept. of Geological Sciences, Studies in Geology 12.

Additional Reading

Conway, Charles, and John H. Weitz, Jr., 1982, Mesoscopic analysis of the Middle Ordovician Tellico-Sevier Shale belts in east Tennessee, GSA Abstracts with Programs, vol. 14, no. 7, p 466.

Donath, Fred A., and Ronald B. Parker, 1964, Folds and Folding, Bulletin Geological Society of America, vol. 75, pp. 45-62.

Engelder, T., and R. Engelder, 1977, Fossil Distortion and decollement tectonics on the Appalachian Plateau: Geology, vol. 5, pp.457-460.

Groshong, Richard H. Jr., 1975, "Slip" cleavage caused by pressure solution in buckle folds, Geology, vol. 3, pp.411-413.

Gwinn, V. E., 1970, Kinematic patterns of lateral shortening, Valley and Ridge Province, Central Appalachians, south-central Appalachians, in Fisher, G. W., et al, eds., Studies of Appalachian Geology--Central and Southern: New York, Wiley Interscience, pp. 127-146.

Harris, L. D., 1970, Details of thin-skinned tectonics in part of the Valley and Ridge and Cumberland Plateau Provinces of the Southern Appalachians, in Fisher, G. W., et al eds., Studies of Appalachian Geology--Central and Southern: New York, Wiley Interscience, pp. 161-173.

Harris, L. D., and K. C. Bayer, 1979, Sequential development of the Appalachian orogen above a master decollement-a hypothesis, Geology, vol. 7, pp. 568-572.

House, W. M., and D. R. Gray, 1982a, Cataclasites along the

Saltville thrust, U.S.A., and their implications for thrust sheet emplacement, Journal of Structural Geology, vol. 4, pp. 252-269.

House, W. M., and D. R. Gray, 1982b, Displacement transfer at a thrust termination in southern Appalachians-Saltville thrust as an example, American Association of Petroleum Geologists Bulletin, vol. 66, pp. 830-842.

Hudleston, P. J., 1972, Fold morphology and some geometrical implications of theories of fold development, Tectonophysics, vol. 16, pp. 1-46.

Hudleston, P. J., 1973, The analysis and interpretation of minor folds developed in the Moine rocks of Mona, Scotland, Tectonophysics, vol. 17, pp. 89-132.

Hudleston, P. J., and T. B. Holzt, 1984, Strain analysis and fold shape in a limestone layer and implications for layer rheology, Tectonophysics, vol. 106, pp.321-347.

King, P. B., and H. W. Ferguson, 1960, Geology of northeasternmost Tennessee, U.S. Geological Survey Prof. Paper 311, 136 p.

Marshak, Stephen, Peter A. Geiser, Walter Alvarez and Terry Engelder, 1982,, Mesoscopic fault array of the northern Umbrian Apennine fold belt, Italy, Geological Society of America Bulletin, vol. 93, pp. 1013-1022.

Nickleson, Richard P., 1972, Attributes of rock cleavage in some mudstones and limestones of the Valley and Ridge Province, Pennsylvania, Geology, vol. 46, pp. 107-112.

Prior, D. J., R. J. Knipe, M. P. Bates and others, 1987, Orientation of specimens: Essential data for all fields of geology, Geology, vol. 15, pp. 829-831.

Ramsay, J. G., 1980, The crack-seal mechanism of rock deformation, Nature, vol. 284, no. 5752, pp. 135-139.

Reks, I. J., and D. R. Gray, 1983, Strain patterns and shortening in a folded thrust belt: an example from the southern Appalachians, Tectonophysics, vol. 91.

Roeder, Eietrich, William Youst, and Robert Little, Folding in the Valley and Ridge Province of Tennessee, American Journal of Science, vol. 278, pp. 477-496.

Rogers, J., 1970, The tectonics of the Appalachians: New York, Interscience Publishers, 271.

Suppe, John, 1983, Geometry and Kinematics of fault bend folding,

American Journal of Science, vol. 283, pp. 684-721.

Suppe, John, and Donald A. Medwedeff, 1984, Fault propagation folding, GSA Abstracts with Programs, vol. 16.